

Uranium-Trend Dating and Calibrations for Quaternary Sediments

by

J. N. Rosholt, C. A. Bush, R. R. Shroba, K. L. Pierce, and G. M. Richmond

U. S. Geological Survey  
Lakewood, Colorado

Open-File Report 85-299  
1985

This report is preliminary and has not been reviewed for conformity with U.S. Geological Survey editorial standards. Any use of trade names is for descriptive purposes only and does not imply endorsement by the USGS.

## ABSTRACT

The findings of the studies presented in this report demonstrate the application and reliability of uranium-trend dating for estimating the time of deposition of a wide variety of surficial deposits, including glacial till, loess, alluvium, colluvium, and altered volcanic ash. For dating of deposits ranging in age from 5,000 to 800,000 years, the open-system technique consists of determining a linear trend from analyses of four to ten channel samples collected at different depths in a given depositional unit or the soil horizons formed in the depositional unit. The concentrations of  $^{238}\text{U}$ ,  $^{234}\text{U}$ ,  $^{230}\text{Th}$ , and  $^{232}\text{Th}$  are accurately determined for each sample. Analyses are made on subsamples of the less than 2 mm-size fraction. Isotopic concentrations are determined by alpha spectrometry utilizing radioisotope dilution techniques. The results of these analyses are plotted as ratios of  $(^{238}\text{U}-^{230}\text{Th})/^{238}\text{U}$  versus  $(^{234}\text{U}-^{238}\text{U})/^{238}\text{U}$ . Ideally, these data points yield a linear array in which the slope of the line of best fit changes predictably for increasingly older deposits. The rate of change of slope is determined by the half-period of uranium flux,  $F(0)$ . An empirical model compensates for differing values of  $F(0)$  in response to climate and other local and regional environmental factors.

Analyses of deposits of known ages are required to calibrate the empirical model; calibrations were provided by correlations with deposits dated by the radiocarbon and K-Ar methods. Deposits used for calibration are alluvium of mid-Holocene age (5Ka) near Denver, loess of late Wisconsin age (12 Ka) in Minnesota, glacial till and loess of Bull Lake age (150 Ka) near West Yellowstone, Montana and till of Bull Lake age (150 Ka) near Pinedale, Wyoming, and zeolitized volcanic ash from Lake Tecopa, California (Tuff A, 600 Ka, and Tuff B, 730 Ka). Tuff A and Tuff B are the distal facies of the Lava Creek ash and the Bishop Tuff, respectively.

At best, the uranium-trend ages have an estimated accuracy of about  $\pm 10$  percent for depositional units between 60,000 and 600,000 years old; however, the uncertainty in the slope is strongly dependent on the quality of the linear trend regarding scatter of data points and the length of the line defined by the points. Analyses of 21 depositional units are discussed in this report; several of these units are calibration points for the model. The ages of these units range from about 5 Ka years for Piney Creek alluvium, to greater than 800 Ka years for altered volcanic ash that has been correlated with the Huckleberry Ridge ash bed (Pearlette Type B ash).

## INTRODUCTION

Uranium-series disequilibrium methods described by Ku and others (1979) used conventional  $^{230}\text{Th}/^{234}\text{U}$  methods for dating pedogenic carbonates which form rinds on alluvial gravel. These ages provide reasonable estimates of the minimum age of the alluvium. A variation of uranium-series dating called uranium-trend has been tested extensively over the past decade. Preliminary models for uranium-trend dating were described by Rosholt (1978, 1980a). Samples for dating were collected from a variety of Quaternary deposits, including alluvium, colluvium, eolian sediments, glacial deposits, and zeolitized volcanic ash. Detailed systematics of the current uranium-trend model are described by Rosholt (1985); therefore, only a brief discussion of the mechanisms of uranium migration in surficial deposits is included in this paper.

After deposition of detrital sediments or geochemical precipitates, they are subject to interactions with materials carried in waters that move through these sediments. Waters that permeate deposits contain at least small amounts of uranium; this uranium decays, producing radioactive daughter products that are readily adsorbed on matrix material, primarily on particles of silt size and finer. If the trail of daughter products,  $^{234}\text{U}$  and  $^{230}\text{Th}$ , are distributed in a systematic pattern, an empirical model for uranium-trend dating can be developed.

Results of other studies of uranium-series disequilibria indicate that uranium commonly exhibits an open-system behavior (Rosholt, 1980b). For conventional uranium-series dating, a closed system exists throughout the history of a deposit if there has been no postdepositional migration of  $^{238}\text{U}$  or of its in-situ produced daughter products,  $^{234}\text{U}$  and  $^{230}\text{Th}$ . However, open-system conditions impose no restrictions on postdepositional migration of these radioisotopes within and between deposits. To meet the requirements for uranium-trend dating, the distribution of associated uranium-series members in the geochemical environment during and after sedimentation must have been controlled by open-system behavior. The large number of geochemical variables in an open system precludes the definition of a rigorous mathematical model for uranium migration. Instead, an empirical approach is used to define the parameters that can reasonably explain the patterns of isotopic distributions. This approach requires independent time calibration and evaluation of the stratigraphic relationships of the deposits.

In the geologic environment, uranium occurs chiefly in two different phases: (1) as a resistate or fixed phase (solids are dominant) where uranium is structurally incorporated in matrix minerals, and (2) as a mobile phase (water is dominant) which includes the uranium flux that migrates through a deposit. This mobile-phase uranium is responsible for an isotopic fractionation process in the  $^{238}\text{U}$ - $^{230}\text{Th}$  series that enables a uranium-trend dating technique to work. Another fractionation process is the preferential leaching of  $^{234}\text{U}$  from the fixed phase. Many of the deposits analyzed in this study probably are slightly moist and typically are not wet or saturated. Nevertheless, uranium migration occurs, perhaps, only seasonally, either in solution or on colloids that slowly move through voids between mineral grains. In arid and semiarid environments, much of the mobile-phase uranium that leaves its trail of daughter products in a deposit (daughter emplacement) actually spends most of its time on the surface of dry mineral grains, and only a small amount of the time is spent in solution or in a suspension moving through a deposit. As a deposit undergoes interstratal alteration, some uranium isotopes are released from the fixed phase and enter the mobile phase; this process results in another form of isotopic fractionation ( $^{234}\text{U}$  displacement).

Analyses of the isotopic abundances of  $^{238}\text{U}$ ,  $^{234}\text{U}$ ,  $^{230}\text{Th}$ , and  $^{232}\text{Th}$  in a single sample do not demonstrate a useful time-related pattern of distribution in an open-system environment. However, analyses of several samples, each of which has slightly different physical properties and slightly different chemical compositions, may provide a useful pattern of distribution of these isotopes. Several samples per unit, from a relatively large number of alluvial, colluvial, glacial, and eolian deposits, must be analyzed to determine if these useful patterns exist. The starting point for the uranium-trend clock is the initiation of movement of waters through the deposit rather than initiation of soil development, although for many deposits both of these processes start at about the same time.

The purpose of this investigation was to develop a model to describe that part of uranium migration whose end product was a predictable change of uranium and thorium isotopic ratios with time. The model should apply to deposits for which good age control exists; deposits of known age provided both the needed time calibration for the model as well as a basis for evaluating the model's reliability. The units used for primary calibration of the model are discussed in this report. They include tills and loess of late

Wisconsin and Bull Lake ages, and zeolitized volcanic ashes correlated with Lava Creek, Bishop, and Huckleberry Ridge ages.

#### EMPIRICAL MODEL

The very long-lived  $^{238}\text{U}$  isotope (half life of  $4.5 \times 10^9$  years) upon radioactive decay, produced long-lived daughter products,  $^{234}\text{U}$  and  $^{230}\text{Th}$ . The half-life of  $^{234}\text{U}$  is 248,000 years; this isotope has a potential as a geochemical tracer in deposits that are as much as 800,000 years old. The half-life of  $^{230}\text{Th}$  is 75,200 years; because of its daughter-parent relations to  $^{234}\text{U}$ , it is a key isotope used in nearly all uranium-series dating models (Ku, 1976).

For surficial deposits, the starting point for the uranium-trend clock is the initiation of movement of water through the sediment rather than initiation of soil development, although both of these processes may start at essentially the same time. The system equilibrium in the parent material is disturbed during transport, and the process of attainment of a new, readjusted, system equilibrium starts in the sediment at the time of deposition. The empirical model incorporates a component called uranium flux,  $F(0)$ . The actual physical significance of  $F(0)$  is not well understood; it is related to the effective flux of uranium through a deposit, which is a function of climate, sediment texture, and the amount of uranium in the mobile phase. In this model, the effect of this flux on isotopic variations decreases exponentially with time. The following is an oversimplified example of the uranium flux in alluvium. At the time of deposition, large volumes of water pass through the alluvium. However, after compaction and during subsequent soil development, the volumes of water passing through the alluvium are reduced significantly. Both the quantity of water passing through and affecting a deposit, and the concentration of uranium in this water are components of the flux; its magnitude is a function of the concentration of uranium in the mobile phase relative to the concentration of uranium in the fixed phase.

Because of the large number of variables in a system that is completely open with regard to migration of uranium, a rigorous mathematical model based on simple equations for radioactive growth and decay of daughter products cannot be constructed. Instead, an empirical model based on results obtained from several alluvial, colluvial, glacial, and eolian deposits of different ages is constructed for the solution of uranium-trend ages. The model

requires calibration of both the uranium-trend slope and the uranium-flux based on results from deposits of known age.

The isotopic composition of several samples from the same depositional unit, expressed in activity units, is required for solution of the model. The trend value from which ages are calculated is the slope of the line representing

$$\frac{\Delta(^{234}\text{U} - ^{238}\text{U})}{\Delta(^{238}\text{U} - ^{230}\text{Th})}$$

To accommodate measured isotopic data, the isotopic variations are normalized to  $^{238}\text{U}$  and the equations for the U-trend model are written in the form of Bateman equations

$$\frac{Y}{X} = \frac{\Delta(^{234}\text{U} - ^{238}\text{U})/^{238}\text{U}}{\Delta(^{234}\text{U} - ^{230}\text{Th})/^{238}\text{U}} \frac{C_1 e^{-\lambda_0 t} + C_2 e^{-\lambda_2 t}}{C_3 e^{-\lambda_0 t} + C_4 e^{-\lambda_2 t} + C_5 e^{-\lambda_3 t}}$$

$$C_1 = \frac{-\lambda_0 \lambda_2}{\lambda_2 - \lambda_0}; \quad C_2 = \frac{\lambda_2 \lambda_2}{\lambda_2 - \lambda_0}; \quad C_3 = \frac{3\lambda_0 \lambda_2 \lambda_3}{(\lambda_2 - \lambda_0)(\lambda_3 - \lambda_0)};$$

$$C_4 = \frac{3\lambda_2 \lambda_2 \lambda_3}{(\lambda_0 - \lambda_2)(\lambda_3 - \lambda_2)} + 2\lambda_2; \quad C_5 = \frac{3\lambda_2 \lambda_3 \lambda_3}{(\lambda_0 - \lambda_3)(\lambda_2 - \lambda_3)} - \lambda_3$$

where  $\lambda_0$  is the decay constant of  $F(0)=\ln 2/[\text{half period of } F(0)]$ ,  $\lambda_2$  is the decay constant for  $^{234}\text{U}$ , and  $\lambda_3$  is the decay constant for  $^{230}\text{Th}$ .

These are empirical model equations and the numerical constants in the coefficients preceding the exponential terms were determined by computer synthesis to provide a model with the best fits for deposits of known age. The alternative uranium-trend slope represented by

$$\frac{Y}{X - Y} = \frac{\Delta(^{234}\text{U} - ^{238}\text{U})/^{238}\text{U}}{\Delta(^{238}\text{U} - ^{230}\text{Th})/^{238}\text{U}}$$

is used for computer solution of the age. An example of this plot is shown in Figure 1.

An additional parameter in the uranium-trend plot is the intercept of the line on the X-axis,  $x_i$ , represented by

$$y = mx + b$$

$$x_i = -b/m$$

where  $m$  is the measured slope of the line,  $b$  is the intercept on the Y-axis, and  $x_i$  is the intercept on the X-axis. The value of  $x_i$  is used to obtain time calibration for the uranium-trend model.

A different plot of the isotopic data can be constructed when the  $^{238}\text{U}/^{232}\text{Th}$  ratios of the samples are plotted on the X-axis versus the  $^{230}\text{Th}/^{232}\text{Th}$  ratios plotted on the Y-axis as shown in Figure 2. This thorium plot is similar to the isochron plot used by Allegre and Condomines (1976) for dating of young volcanic rocks. The plot is used to determine if all the samples included in the uranium-trend line describe a reasonable linear array on the thorium plot, and thus serves as a useful check to determine if all samples belong to the same depositional unit.

The half period of  $F(0)$  and its decay constant,  $\lambda_0$ , are strictly empirical values which allow selection of the proper exponential coefficient in the equation for the uranium-trend model. For depositional units of unknown age, a method is required to determine the proper decay constant to be used in the equation; this is determined with a calibration curve based on  $\lambda_0$  established for units of known age. For this calibration, the quantity  $x_i$  is plotted against the half period  $F(0)$  on the log-log plot shown in Figure 3.

#### CALIBRATION

Analyses of units of known age are needed for time calibration of the empirical model. The calibration curve is determined by selecting the proper  $\lambda_0$  value that will yield the known age for a depositional unit using the model equation. The  $x_i$  values of known-age deposits are used for calibration and these values are plotted against the half periods of  $F(0)$  equivalent to their  $\lambda_0$  values. The quantity, half period of  $F(0)$ , is one variable used for calibration of the model, and the value,  $x_i$ , is the measured parameter in the calibration. Units of known age used for calibration points that define the line are indicated on Figure 3; the unit number and age are included for each calibration point.

## LOCATIONS, UNIT AND SECTION DESCRIPTIONS, AND URANIUM-TREND AGES

In this report, the deposit or vertical sequence of deposits sampled for uranium-trend dating at a given locality are referred to as either a unit (depositional unit) or a section, respectively. A unit consists of one or more deposits, of similar or different origin, that are considered to be of similar age; a section consists of two or more units.

### Unit PC

Soil developed in Piney Creek Alluvium of Holocene age described by Scott (1963, p. 43) was collected by J. N. Rosholt in 1965 on the east side of a gully near the Hogback in the SW 1/4, NW 1/4 sec. 2, T.7S., R.69W., Kassler quadrangle, Jefferson County, Colorado. The independent age of this deposit is approximately 5 Ka years (Scott, 1963, p. 52). The plots of 5 samples from this unit are shown in Figure 4. The uranium-trend line yielded an age of  $5 \pm 20$  Ka.

### Unit WF

The analytical data and description of this unit are taken from Rosholt and others (1966). This unit consists of soil developed in loess and unweathered loess of late Wisconsin age in Wabasha County, Minnesota. Plots of the lower 6 samples in this unit are shown in Figure 5. Data from the sample of the A horizon was not included in the linear trend because the upper part of this sample was collected within 8 cm of the surface. The independent age estimate of this deposit is 12 Ka (Frye, 1973). This unit is one of the calibration points (Unit 2, Fig. 3); it has a uranium-trend age of  $7 \pm 5$  Ka.

### Unit FF

The analytical data and description of this unit are taken from Rosholt and others (1966). This unit consists of a soil developed in loess and unweathered loess of late Wisconsin age in Fillmore County, Minnesota. Plots of the lower 5 samples in this unit are shown in Figure 6. The uppermost sample of A2 horizon was excluded from the slope calculation because of its shallow depth below surface. The independent age estimate of this deposit is 12 Ka (Frye, 1973). The uranium-trend age for the lower 5 samples is  $12 \pm 15$  Ka.

#### Unit K

The analytical data and description of this unit are taken from Rosholt and others (1966). The unit consists of a soil developed in till of late Wisconsin age in Mower County, Minnesota. Plots of the lower 4 samples in this unit are shown in Figure 7. Because of its shallow depth, the A horizon was not included in the uranium-trend line which gave an age of  $15 \pm 15$  Ka.

#### Unit MSV1

This unit consists of a soil developed in slopewash and till, and unweathered till of the Pinedale glaciation. It was collected in the valley of Middle St. Vrain Creek by J. N. Rosholt and R. R. Shroba in 1983 from a back-hoe pit in the SW 1/4, SW 1/4 sec. 18, T.2N., R.72W., Allen's Park quadrangle, Boulder County, Colorado. Three types of deposits are included in this unit that was exposed in the 2.5-meter deep pit. The isotopic data for this unit (Fig. 8) indicate two different linear regression lines; one for the slope wash and the upper, more sandy till and one for the lower, more silty till. The resulting uranium-trend ages are  $12 \pm 14$  Ka for the upper part of the unit and  $60 \pm 50$  Ka for the lower part. The uppermost sample of the lower part of the unit (MSV1-8) was excluded from the uranium-trend plot because, based on element concentrations and isotopic ratios, this sample appears to be a mixture of the two till deposits. It is likely that these two till deposits are the products of the same advance, therefore, they are considered to be of equivalent age.

#### Unit NSV2

This unit consists of a soil developed in till and associated glaciofluvial sand of the Bull Lake glaciation (Madole and Shroba, 1979). It was collected by R. R. Shroba and J. N. Rosholt in 1982 from a hand-dug soil pit described by Shroba and Madole (1979) in NE 1/4, SW 1/4 sec 23, T.3N., R.73W., Allen's Park 7 1/2' quadrangle, Boulder County, Colorado. The uranium-trend age for the till is  $130 \pm 80$  Ka (Fig. 9). This unit is used as a secondary confirmation for the calibration curve.

#### Unit FD

This sequence of samples was collected by G. M. Richmond and C. J. Sorenson in 1983 from the outer Bull Lake moraine at Fremont Lake near Pinedale in Sublette County, Wyoming (Richmond, 1973). Eight samples were

collected at 30 cm intervals from till in the west wall of Fremont Ditch in in NW 1/4, NW 1/4 sec. 35, T.34N., R.109W., Fremont Lake South quadrangle. No soil profile is preserved in the till which is disconformably overlain by 0.5 m of colluvium that was not sampled. The plots shown in Figure 10 yield an age of  $160 \pm 50$  Ka.

#### Unit P78

This unit consists of a soil developed in till of the Bull Lake glaciation (Pierce and others, 1976). It was collected in a soil pit 16 km north of West Yellowstone, Montana by K. L. Pierce in 1975 near the obsidian-hydration locality 2 of Pierce and others (1976, p. 407) in NE 1/4, NE 1/4, NE 1/4, sec. 15, T.12S., R.5E., Tepee Creek quadrangle, Gallatin County, Montana. This unit is older than the West Yellowstone flow which has a K-Ar age of  $117 \pm 8$  Ka (J. D. Obradovich, written commun. cited in Pierce, 1979, p. F23). Obsidian-hydration studies, calibrated by K-Ar dating, indicate an age of  $150 \pm$  approximately 15 Ka (K. L. Pierce, written commun., 1980). This deposit is used as one of the calibration points (unit 7, Fig. 3). The slope, including only the upper 4 samples, is shown in Figure 11; the lowermost sample, P75-78Q, is from the underlying unit. The uranium-trend age for the till is  $150 \pm 100$  Ka.

#### Unit P79

This unit consists of a soil developed in till of the Pinedale glaciation (Pierce and others, 1976). It was collected 9 km east of West Yellowstone, Montana by K. L. Pierce in 1975 near obsidian-hydration locality 7 of Pierce and others (1976, p. 704) at  $44^{\circ}40'N.$ ,  $111^{\circ}59'W.$  in Madison Junction quadrangle, Gallatin County, Montana in Yellowstone National Park. This unit could not be dated by the uranium-trend model because all samples analyzed plot very close to the radioactive-equilibrium point as shown in Figure 12. The till parent material was derived from Quaternary rhyolite, which initially contained more uranium than do other more typical alluvial deposits and probably contained excess fixed-phase uranium relative to the amount of mobile-phase uranium contained in pore waters.

#### Section P183

This section consists of a soil developed in loess of the Pinedale glaciation and a buried soil formed in loess and kame gravel of the Bull Lake

glaciation. It was collected in a backhoe pit by K.L. Pierce and M. Fosberg (University of Idaho) in 1978 along the South Fork of the Madison River, 12 km northwest of West Yellowstone, Montana in NE 1/4, SW 1/4, SW 1/4, sec. 3, T.12S., R.4E., West Yellowstone quadrangle, Gallatin County, Montana. The upper unit is a 72 cm thick soil formed in loess of the Pinedale glaciation. It was not datable with the uranium-trend model because there is very little spread on the trend line (Fig. 13) and little variation in the  $^{234}\text{U}/^{238}\text{U}$  ratios in the suite of samples. The lower unit is a buried soil developed in loess and kame gravel of the Bull Lake glaciation. It has age control provided by the combined K-Ar and obsidian hydration methods of about 150 Ka (Pierce, 1979, p. F24). The bottom sample in this section kame gravel of Bull Lake age, was not included in the trend line (Fig. 14) because it does not plot near the other samples on the Th-index plot. The lower unit of this section is used as a calibration point (Unit 8, Fig. 3); it has a uranium-trend age of  $160 \pm 50$  Ka.

#### Unit P184

This is a soil developed in till of the Bull Lake glaciation. It was sampled from a backhoe pit 1.9 km northeast of the Duck Creek "Y", 14.6 km north of West Yellowstone, Montana, by K. L. Pierce and M. Fosberg in 1978 in NE 1/4, NE 1/4, NE 1/4 sec. 15, Tepee Creek quadrangle, Gallatin County, Montana. The till is mantled by thin loess thought to be of Pinedale age. Samples with pedogenic silica define better fits on the straight-line plots than the other samples. The uranium-trend line (Fig. 15) indicates an age of  $190 \pm 90$  Ka for the lowermost 6 samples that contain pedogenic silica.

#### Unit Tuff A

The samples of tuff A from Lake Tecopa, Inyo County, California were provided by A. J. Gude. Sample locations and descriptions are given in Sheppard and Gude (1968, Table 10 and Fig. 13, localities 5 and 6). Tuff A has been correlated by Izett and others (1970) with the Pearlette type 0 ash or Lava Creek ash that has a K-Ar age of 0.6 Ma. This unit is used as a calibration point (unit 11, Fig. 3); it has a uranium-trend age of  $600 \pm 60$  Ka. Two samples containing uraniferous opal (T5E and T6B) were excluded from the plots shown in Figure 16.

#### Unit Tuff B

The samples of tuff B from Lake Tecopa, Inyo County, California were provided by A. J. Gude. Sample locations and descriptions are presented in Sheppard and Gude (1968, Table 10, Fig. 14, as locality 128). Sample 128B listed in tables of Sheppard and Gude (1968) was not available for analysis; however, sample 128A was available. Sample 128A contains 90-95 percent phillipsite and trace amounts of calcite, feldspar, clay, and quartz (A. J. Gude, oral commun., 1978). Tuff B has been correlated by Izett and others (1970) with the Bishop Tuff which has a K/Ar age of 0.73 Ma. This unit, with plots shown in Figure 17, was used for a calibration point (Unit 12, Fig. 3); it has a uranium-trend age of  $740 \pm 100$  Ka.

#### Unit Tuff C

The samples of tuff C from Lake Tecopa, Inyo County, California, were provided by A. J. Gude. Sample locations and descriptions are listed in Sheppard and Gude (1968, Table 10 and Fig. 15 locality 122). Tuff C has been correlated by Izett and others (1970) with the Pearlette type B ash or Huckleberry Ridge ash bed which has K/Ar ages of about 1.9 Ma. Plots of this unit are shown in Figure 18. It has a uranium-trend age greater than 800 Ka. owing to the uncertainty deducted from the measured slope which yields a minimum value of 800 Ka.

#### Unit CCA

This unit is a soil developed in alluvium of unknown age. It was collected by J. N. Rosholt in 1969 as part of an investigation of leaching of uranium from granitic rocks. The alluvium exposure was on the west side of a stream cut of Corral Creek on the southeastern flank of the Shirley Mountains in the NE 1/4, NE 1/4 sec. 25, T.25N., R.83W., Schneider Ridge quadrangle, Carbon County, Wyoming. Plots of the isotopic ratios, which have a nearly ideal spread on the trend line, are shown in Figure 19. The uranium-trend age for this deposit is  $60 \pm 6$  Ka.

#### Section NSV3

This section consists of a soil developed in colluvium and a buried soil developed in mixed loess and pre-Bull Lake till (Madole and Shroba, 1979). It was collected from a soil pit near the mouth of North St. Vrain Creek by R. R. Shroba and J. Rosholt in 1982. The upper unit was sampled from the south face and the lower unit was sampled from the north face of the soil pit in SE 1/4,

NE 1/4 sec 14, T.3N., R.73W., Allen's Park quadrangle, Boulder County, Colorado. The plot of the upper unit (Fig. 20) yields a uranium-trend age of  $220 \pm 70$  Ka. No age could be calculated for the lower unit owing to the small variation in  $^{234}\text{U}/^{238}\text{U}$  ratios for all of the samples (Fig. 21).

#### Section GF

This section consists of a soil developed in younger colluvium, older colluvium, and volcanic ash. It was collected from a trench across the Golden fault, 1.2 km northwest of downtown Golden by J. N. Rosholt, G. R. Scott, and B. J. Szabo in the NE 1/4, SW 1/4 sec. 28, T.3S., R.70W. An illustration of the exposure is shown in Kirkham (1977, Fig. 4); it is the upper portion above the ledge in the center of the photograph. Uranium-trend results indicate that there are two colluvial units. The upper unit dated at  $190 \pm 60$  Ka and the lower unit at  $440 \pm 90$  Ka. The sample containing reworked ash and silt (GF-8) did not plot near the other data points on the Th-index plot or the U-trend plot shown in Figure 22. Comparison of the impure ash sample with clean ash (Sample 76G27 provided by G. A. Izett) from an exposure west of the Section GF suggest that the ash in Section GF is reworked and is older than the lower silt unit that contains the ash.

### RESULTS

Analyses of samples from 21 units are included in this report. Unit and section locations, soil data, sample depths, and uranium and thorium content for each sample are listed in Table 1. Uranium and thorium element concentrations are precise within  $\pm 2$  percent. Of the 21 depositional units, three (P75-79, P78-183 upper unit, and NSV3 lower unit) are not datable using the uranium-trend model described. Two of the undatable units are loess or till of late Wisconsin age; and the other is till of pre-Bull Lake age. The isotopic ratios used for the plots are listed in Table 2. The 2 standard deviation error values required for computer calculation of the slope and uncertainty of the slope of the linear regression line are included with the isotopic ratios in Table 2. An additional significant figure for these data (Table 2) is retained for the slope calculation to avoid premature arithmetic rounding. Uranium-trend and thorium plots for each depositional unit (Table 1) are shown in Figs. 4 through 22.

As noted earlier, some data were not included in the uranium-trend age calculations. Some of the units sampled and analyzed in the early phase of

this investigation included near-surface material at depths of less than 8 cm. Data from these near-surface samples have been excluded from the calculation of the linear regression line because of the likelihood of contamination by dust and other foreign material. In other cases, samples were excluded from the uranium-trend line if, on the thorium plot, they did not conform to the linear array displayed by the other samples in the deposit. One reason for a departure from linearity is that the sample belongs to a different age deposit or it contains a significant component of material from a different deposit. This problem usually is encountered only with the uppermost or lowermost samples in a deposit. Another reason for these discrepancies is that the porosity and permeability characteristics of layers in the same depositional unit may be sufficiently different to result in very different effective uranium fluxes. For instance, the effective flux is different for an open-work gravel where the mobile-phase uranium has a short residence time compared to that in a clayey layer through which fluids move slowly with time. Assimilation of uranium during later stages of alteration of a deposit can cause anomalous variations in the isotopic system such as in the incorporation of uraniferous opal. Examples of these anomalous variations include: a buried till below the B horizon (sample P75-78Q) and the kame gravel (sample P78-183-12) of Bull Lake age (Figs. 11 and 14); the upper three samples (P78-184-1, 2, 3) of till of the Bull Lake age (Fig. 18) that do not contain authigenic silica as do the other samples in the sections; uppermost sample (NSV3U-1) of section NSV3 (Fig. 20); the ash-bearing horizon (sample GF-8) of section GF (Fig. 21); and the samples containing uraniferous opal (T5E and T6B) in tuff A at Lake Tecopa (Fig 16). On the basis of the fit of the data on the thorium plot, samples can be identified that do not belong to the same depositional unit or that have mineralogy and grain size that are unlike those of the other samples in the unit.

A summary of model parameters for the 17 dated units is shown in Table 3, which includes the values for X-intercept, half period of  $F(0)$ , uranium-trend slope, and age for each unit. The uncertainty in each age listed is one standard deviation including scatter as defined by Ludwig (1979). A unit number for each dated deposit is included in Table 3; corresponding unit numbers of those units used to define the calibration curve are included in Figure 3.

## CONCLUSIONS

Uranium-trend dating is useful to estimate the age of Quaternary deposits and the best accuracy appears to be in the range of 60,000 to 600,000 years which at best may be  $\pm 10$  percent for units that have a well defined linear trend and minimum scatter about the uranium-trend slope. Errors well in excess of 10 percent are encountered near the lower and upper limits of the age range of the method. Age resolution in deposits less than 20,000 years old have errors near or greater than 100 percent of the age value. The error with respect to the maximum age of deposits greater than 600,000 years usually is greater than 20 percent and the limit on the possible maximum age becomes uncertain for ages greater than 700,000 years. Dating of deposits in Nevada and New Mexico (J. N. Rosholt, unpublished data) indicate that chronology resolution is better for calcareous deposits than for noncalcareous deposits such as most glacial tills and loess. Alluvial deposits which tend to be more poorly sorted and of mixed mineralogy usually yield a better spread of the data on the uranium-trend plot than do eolian or quartz rich sand deposits that have minimal soil development.

With the following examples, uranium-trend systematics indicate that:

(1) The dates obtained for till units in Colorado confirm ages based on field data:

Pinedale =  $60 \pm 50$  Ka.

Bull Lake =  $130 \pm 80$  Ka.

pre-Bull Lake =  $220 \pm 70$  Ka.

These show agreement with West Yellowstone tills and give strength to the idea that the uranium-trend model can be used for long-distance correlation.

(2) Uranium-trend plots can identify multiple units within one stratigraphic section (Fig. 22).

(3) Uranium-trend plots can identify mineralogic differences in uranium behavior (Fig. 14, Fig. 16).

## REFERENCES CITED

- Allegre, C. J., and Condomines, M., 1976, Fine chronology of volcanic processes using  $^{238}\text{U}/^{238}\text{Th}$  systematics: Earth and Planetary Science Letters, v. 28, p. 395-406.
- Frye, J. C., 1973, Pleistocene succession of the central interior United States: Quaternary Research, v. 3, p. 275-283.
- Izett, G. A., Wilcox, R. E., Powers, H. A., and Desborough, G. A., 1970, The Bishop ash bed, a Pleistocene marker bed in the Western United States: Quaternary Research, v. 1, p. 122-132.
- Kirkham, R. M., 1977, Quaternary movements on the Golden Fault, Colorado: Geology, v. 5, p. 689-692.
- Ku, T. L., 1976, The uranium-series methods of age determination: Annual Rev. Earth and Planetary Science Letters: v. 4, p. 347-349.
- Ku, T. L., Bull, W. B., Freeman, S. T., and Knauss, K. G., 1979,  $\text{Th}^{230}\text{-U}^{234}$  dating of pedogenic carbonates in gravelly desert soils of Vidal Valley, Southeastern California: Geol. Soc. America Bull., v. 90, p. 1063-1073.
- Madole, R. F., and Shroba, R. R., 1979, Till sequence and soil development in the North St. Vrain drainage basin, east slope, Front Range Colorado, in Ethridge, F. G., (ed), Field guide northern Front Range and northwest Denver Basin, Colorado: Geol. Soc. America Rocky Mtn. Sec. Ann. Meeting, 32nd, Fort Collins, p. 124-178.
- Pierce, K. L., 1979, History and dynamics of glaciation in the northern Yellowstone National Park area: U. S. Geol. Survey Prof. Paper, 729F, p. F1-F90.
- Pierce, K. L., Obradovich, J. D., and Friedman, I., 1976, Obsidian hydration dating and correlation of Bull Lake and Pinedale glaciations near West Yellowstone, Montana: Geol. Soc. America Bull., v. 87, p. 702-710.
- Richmond, G. M., 1973, Geologic map of the Fremont Lake South quadrangle, Sublette County, Wyoming: U.S. Geol. Survey Geologic Quadrangle Map GQ-1138.
- Rosholt, J. N., 1978, Uranium-trend dating of alluvial deposits: in Short Papers of the Fourth Internat. Conf., Geochronology, Cosmochronology, and Isotope Geology, U. S. Geol. Survey Open-File Report 78-701, p. 360-362.
- Rosholt, J. N., 1980a, Uranium-trend dating of Quaternary sediments: U. S. Geol. Survey Open-File Report 80-1087, 65 p.
- Rosholt, J. N., 1980b, Uranium and thorium disequilibrium in zeolitically altered rock: Nuclear Technology, v. 57, p. 143-146.
- Rosholt, J. N., 1985, Uranium-trend systematics for dating Quaternary deposits: U.S. Geol. Survey Open-File Report 85-298, 34 p.

- Rosholt, J. N., Doe, B. R., and Tatsumoto, M., 1966, Evolution of the isotopic composition of uranium and thorium in soil profiles: Geol. Soc. America Bull., v. 77, p. 987-1004.
- Scott, G. R., 1963, Quaternary geology and geomorphic history of the Kassler quadrangle, Colorado: U. S. Geol. Survey Prof. Paper 421A, 70 p.
- Sheppard, R. A., and Gude, A. J., 1968, Distribution and genesis of authigenic silicate minerals in tuffs of Pleistocene Lake Tecopa, Inyo County, California: U. S. Geol. Survey Prof. Paper 597, 38 p.

Table 1. Depths, soils data, uranium and thorium concentrations, and Th/U ratios for alluvial, colluvial, glacial, and eolian deposits

Sample number	Depth (cm)	Soil Data		U (ppm)	Th (ppm)	Th/U
		Horizon	Comments			
Unit PC, Jefferson County, Colorado. Soil developed in Piney Creek alluvium of Holocene age.						
PC-1	8-38	A	humic silt	2.39	8.64	3.61
PC-2	38-53	B	silt	1.95	6.83	3.51
PC-3	53-76	B	silt	1.95	7.56	3.88
PC-4	76-102	C	silt	2.23	8.62	3.87
PC-5	102-122	C	silt	2.22	10.5	4.73
Unit WF, Wabasha County, Minnesota. Soil developed in loess of late Wisconsin age.						
WF-1	1-20	A		2.33	8.46	3.64
WF-2	30-61	B		2.66	9.91	3.73
WF-3	61-91	B		2.49	9.61	3.86
WF-4	91-122	B		2.37	9.37	3.95
WF-5	122-152	C		2.21	8.26	3.74
WF-6	152-178	C		2.20	8.00	3.64
WF-7	178-213	C		2.04	7.58	3.72
Unit FF, Fillmore County, Minnesota. Soil developed in loess of late Wisconsin age.						
FF-1	1-23	A2		3.17	9.30	2.93
FF-2	23-53	B1		3.22	10.2	3.16
FF-3	53-84	B21		3.27	10.6	3.25
FF-4	84-119	B22		3.07	10.4	3.39
FF-5	119-285	C1		3.03	10.5	3.46
FF-6	285-310	C2		2.57	8.13	3.16
K unit, Mower County, Minnesota. Soil developed in till of late Wisconsin age.						
K-1	0-20	A		3.24	8.30	2.56
K-2	20-56	B1		3.45	8.61	2.49
K-3	56-91	B2		2.18	8.13	3.73
K-4	84-152	C1		1.92	7.94	4.13
K-5	152-178	C2		2.06	7.59	3.69
Unit MSV1, Boulder County, Colorado. The upper part of this unit is developed in slopewash and in sandy till of the Pinedale glaciation; the lower part is unweathered, silty till of the Pinedale glaciation.						
<u>Upper part</u>						
MSV1-1	30-40	A1		1.96	19.1	5.16
MSV1-2	40-55	2B21t		2.23	14.7	6.60
MSV1-3	55-70	2B21t		1.93	9.53	4.94
MSV1-4	70-85	2B22t		2.06	13.5	6.54
MSV1-5	85-100	2B22t		2.91	18.1	6.22
MSV1-6	100-125	2Cox		2.16	12.6	5.82
MSV1-7	125-150	2Cox		2.23	14.3	6.40

Table 1. Depths, soils data, uranium and thorium concentrations, and Th/U ratios for alluvial, colluvial, glacial, and eolian deposits (cont'd)

Sample Number	Depth (cm)	Soil Data		U (ppm)	Th (ppm)	Th/U
		Horizon	Comments			
<u>Lower part</u>						
MSV1-8	150-167	3Cn		3.36	19.9	5.93
MSV1-9	167-183	3Cn		4.72	18.8	3.99
MSV1-10	183-200	3Cn		4.49	18.3	4.07
MSV1-11	200-215	3Cn		4.44	16.6	3.74
MSV1-12	215-230	3Cn		5.38	17.6	3.28
MSV1-13	230-245	3Cn		5.21	21.4	4.09
Unit NSV2 , Boulder County, Colorado. Soil developed in till of the Bull Lake glaciation.						
NSV2-1	5-25	A2		1.09	7.32	6.74
NSV2-2	25-60	A2		1.75	11.7	6.67
NSV2-3	60-80	B21t		2.42	17.5	7.22
NSV2-4	80-100	B21t		2.26	13.8	6.09
NSV2-5	100-120	B22t		2.65	19.7	7.43
NSV2-6	120-135	B22t		2.69	18.8	7.01
NSV2-7	135-155	B3		2.36	15.7	6.64
NSV2-8	155-175	C1ox		2.79	16.6	5.96
NSV2-9	175-195	C1ox		2.21	13.6	6.18
NSV2-10	195-210	C2ox		2.32	14.3	6.18
Unit FD, Sublette County, Wyoming. Unweathered till of the Bull Lake glaciation.						
FD-1	30-60	2Cn		1.29	11.0	8.52
FD-2	60-90	2Cn		1.40	10.6	7.58
FD-3	90-130	2Cn		1.61	14.0	8.71
(Lower part of the sampling was offset 3 m to the south to avoid a slump)						
FD-4	90-130	3Cn		1.59	11.7	7.36
FD-5	130-160	3Cn		1.65	12.2	7.39
FD-6	160-190	3Cn		1.69	12.9	7.63
FD-7	190-220	3Cn		1.58	13.4	8.44
FD-8	220-250	3Cn		1.58	13.2	8.36
Unit P75-78, Gallatin County, Montana. Soil developed in till of the Bull Lake glaciation.						
P75-78 M	35-43	2B12		2.68	13.5	5.06
78 N	57-67	2B21		2.68	15.6	5.83
78 O	70-76	2B21		2.41	15.1	6.27
78 P	100-105	2B22		2.57	15.0	5.84
78 Q	125-130	3Cn		2.68	16.3	6.07
Unit P75-79, Gallatin County, Montana. Soil developed in till of the Pinedale glaciation.						
P75-79 F	2-7	B		2.78	12.2	4.40
79 G	15-20	C1ox		3.23	14.4	4.47
79 H	30-37	C2ox		3.28	15.9	4.85
79 I	65-80	C3ox		3.72	19.5	5.25

Table 1. Depths, soils data, uranium, and thorium concentrations, and Th/U ratios for alluvial, colluvial, glacial, and eolian deposits (cont'd)

Sample number	Depth (cm)	Soil Data		U (ppm)	Th (ppm)	Th/U
		Horizon	Comments			
Section P78-183, Gallatin County, Montana. The upper unit is a soil developed in loess of the Pinedale glaciation; the lower unit is a buried soil developed in loess of the Bull Lake glaciation and the underlying kame gravel of the Bull Lake glaciation.						
<u>Upper unit</u>						
P78-183-1	7-9	A11		2.84	12.8	4.51
183-2	19-24	A12		3.05	13.8	4.51
183-3	30-35	B1		3.03	13.5	4.46
183-4	50-55	B2		3.07	13.8	4.49
183-5	68-72	B3		3.11	13.5	4.35
<u>Lower unit</u>						
P78-183-6	75-80	2A21		2.88	13.9	4.82
183-7	90-95	2A22		2.56	12.1	4.74
183-8	100-105	2B1		2.70	14.5	5.37
183-9	120-125	2B21tb		2.57	14.0	5.46
183-10	130-135	2B21tb		2.57	13.2	5.14
183-11	150-155	2B21tb		2.04	11.1	5.45
183-12	165-170	3Cox	Kame gravel	2.72	18.6	6.84
Unit P-78 184, Gallatin County, Montana. Soil developed on till of the Bull Lake glaciation.						
P78-184-1	57-62	2B21tb		3.01	16.9	5.61
184-2	82-87	2B22tb		2.90	16.6	5.72
184-3	100-105	2B22tb		2.78	17.7	6.35
184-4	115-129	2B31tbsi		2.23	13.8	6.17
184-5	120-125	2B31tbsi		2.91	19.7	6.76
184-6	135-140	2B32tbsi		2.24	15.1	6.74
(Samples P78-184-7 through P78-184-9 were collected at the other end of the backhoe pit)						
P78-184-7	123-128	3Cn	sandy channel	3.23	19.1	5.91
184-8	169-174	3Cn	silica layer	2.93	19.3	6.60
184-9	180-185	3Cn	till	2.11	14.1	6.70
Unit Tuff A, Lake Tecopa, Inyo County, California. Samples locations are those of Sheppard and Gude (1968, fig. 13, table 10).						
	<u>Depth above base</u>					
T5 E	330 cm		glass, zeolite and uraniferous opal	5.97	21.2	3.55
T5 D	320 cm		glass and zeolite	5.33	21.4	4.01
T5 C	165 cm		glass and zeolite	5.49	18.9	3.44
T5 B	15 cm		glass	5.85	25.8	4.41
T5 A	at base		zeolite	3.40	7.42	2.18
T6 E	at top		glass and zeolite	4.80	16.7	3.48
T6 D	122 cm		glass	5.90	18.2	3.08
T6 C	61 cm		glass and zeolite	5.92	19.1	3.22
T6 B	41 cm		glass, zeolite and uraniferous opal	16.2	10.9	.67
T6 A	at base		zeolite	3.50	10.2	2.91

Table 1. Depths, soils data, uranium and thorium concentrations, and Th/U ratios for alluvial, colluvial, glacial, and eolian deposits (cont'd)

Sample number	Depth (cm)	Soil Data		U (ppm)	Th (ppm)	Th/U
		Horizon	Comments			
Tuff B, Lake Tecopa. Localities from Sheppard and Gude (1968, fig. 14, table 10).						
T128 D	at top		zeolite	3.59	7.85	2.19
T128 C	at middle		glass	6.38	18.8	2.95
T128 A	at lower part		zeolite	1.61	3.20	1.99
T148 M	at base		glass and zeolite	4.26	12.5	2.95
Tuff C, Lake Tecopa. Localities from Sheppard and Gude (1968, fig. 15, table 10).						
T122 C	at top		clay and zeolite	2.17	21.2	9.79
T122 B	at middle		halite and zeolite	1.15	9.18	8.00
T122 A	at base		zeolite and clay	2.87	29.2	10.2
CCA section, alluvium in stream cut of Corral Creek in NE-1/4, sec. 25, N.25N., R.83W., Schneider Ridge quadrangle, Carbon County, WY.						
CCA-1	8-30	A	silt	3.32	15.0	4.52
CCA-2	30-76	B	silt	4.95	14.9	3.02
CCA-3	76-83	B	humic silt	5.64	17.7	3.14
CCA-4	83-122	C	silt	3.95	15.5	3.92
CCA-5	122-152	C	silt	3.59	17.8	4.96
Section NSV3, Boulder County, Colorado. The upper unit consists of a soil developed in colluvium (U) and the underlying 2A2 horizon formed in loess mixed with till (M). The lower unit is a buried soil developed in mixed loess (M) and pre-Bull Lake till (L). This section was collected in a hand dug soil pit described by Shroba and Madole (1979)						
<u>Upper unit</u>						
NSV3U-1	8-25	A2		2.50	12.0	4.80
NSV3U-2	25-40	A2		1.95	10.7	5.46
NSV3U-3	40-47	B2		3.53	21.3	6.03
NSV3U-4	47-54	B2		3.45	14.6	4.24
NSV3U-5	54-60	B2		2.75	13.8	5.03
NSV3U-6	60-70	Cox		1.69	9.6	5.64
NSV3M-1	70-85	2A2b		4.39	24.5	5.64
<u>Lower unit</u>						
NSV3M-2	67-80	2A2b		4.99	24.5	4.92
NSV3L-1	80-95	3B21tb		3.42	19.2	5.60
NSV3L-2	95-110	3B21tb		3.39	19.4	5.74
NSV3L-3	110-126	3B22tb		4.63	34.9	7.53
NSV3L-4	126-142	3B22tb		2.29	13.7	5.99
NSV3L-5	142-165	3C11oxb		2.88	10.5	3.63
NSV3L-6	165-190	3C11oxb		3.32	13.4	4.04
NSV3L-7	190-210	3C12oxb		6.84	12.6	1.84
NSV3L-8	210-230	3C12oxb		13.1	12.4	.95

Table 1. Depths, soils data, uranium and thorium concentrations, and Th/U ratios for alluvial, colluvial, glacial, and eolian deposits (cont'd)

Sample number	Depth (cm)	Soil Data		U (ppm)	Th (ppm)	Th/U
		Horizon	Comments			
Section GF. Jefferson County, Colorado. The upper unit is a soil developed in colluvium. The lower unit consists of the lower part of the colluvium and volcanic ash.						
GF-1	8-20	A		1.98	13.4	6.75
GF-2	20-40	B		1.93	14.2	7.34
GF-3	40-70	B		2.03	14.6	7.19
GF-4	70-100	Cca		1.97	14.3	7.29
GF-5	100-130	Cca		1.86	13.6	7.29
Lower unit, collected directly below upper unit						
GF-6	130-160		silty colluvium	2.50	14.6	5.82
GF-7	160-180		silty colluvium	2.10	14.7	7.01
GF-8	180-200		silty with ash	2.58	36.0	14.0
GF-9	200-240		silty colluvium	2.07	14.1	6.84
76G27	~400		clean ash	7.31	30.6	4.19

Table 2. Isotopic ratios of uranium and thorium required for U-trend plots

Sample	U ppm	Activity Ratios					
		$\frac{^{234}\text{U}}{^{238}\text{U}}$	$\frac{^{230}\text{Th}}{^{238}\text{U}}$	$\frac{^{238}\text{U}}{^{232}\text{Th}}$	$\frac{^{230}\text{Th}}{^{232}\text{Th}}$	$\frac{(^{238}\text{U}-^{230}\text{Th})}{^{238}\text{U}}$	$\frac{(^{234}\text{U}-^{238}\text{U})}{^{238}\text{U}}$
PC unit (figure 4)							
PC-1	2.39	1.108	1.461	0.828±.043	1.210±.034	-0.461±.061	+0.108±.035
PC-2	1.95	1.136	1.530	.852±.044	1.304±.036	- .530±.064	+ .136±.036
PC-3	1.95	1.120	1.655	.771±.040	1.276±.036	- .655±.071	+ .120±.035
PC-4	2.23	1.115	1.318	.772±.040	1.017±.028	- .318±.055	+ .115±.035
PC-5	2.22	1.026	1.530	.630±.033	.964±.027	- .530±.064	+ .026±.033
WF unit (figure 5)							
WF-1	2.33	.937	1.333	.804±.042	1.072±.030	- .333±.056	- .063±.030
WF-2	2.66	.903	1.433	.781±.041	1.119±.031	- .433±.060	- .097±.029
WF-3	2.49	.909	1.467	.756±.039	1.109±.031	- .467±.062	- .091±.029
WF-4	2.37	.902	1.514	.738±.038	1.118±.031	- .541±.064	- .098±.029
WF-5	2.21	.906	1.417	.780±.041	1.105±.031	- .417±.060	- .094±.029
WF-6	2.20	.915	1.396	.804±.042	1.123±.031	- .396±.059	- .085±.029
WF-7	2.04	.909	1.352	.786±.041	1.063±.030	- .352±.057	- .091±.029
FF unit (figure 6)							
FF-1	3.17	.947	1.293	.995±.052	1.286±.036	- .293±.054	- .053±.030
FF-2	3.22	.922	1.409	.921±.048	1.297±.036	- .409±.059	- .078±.029
FF-3	3.27	.908	1.418	.901±.047	1.277±.036	- .418±.060	- .092±.029
FF-4	3.07	.891	1.427	.860±.044	1.227±.034	- .427±.060	- .109±.029
FF-5	3.03	.928	1.465	.842±.044	1.233±.034	- .465±.061	- .072±.030
FF-6	2.57	.926	1.283	.924±.048	1.185±.033	- .283±.054	- .074±.030
K unit (figure 7)							
K-1	3.24	.993	1.129	1.143±.059	1.290±.036	- .129±.047	- .007±.032
K-2	3.45	.977	1.163	1.170±.061	1.361±.038	- .163±.049	- .023±.031
K-3	2.18	.869	1.192	.784±.041	.953±.026	- .192±.050	- .131±.028
K-4	1.92	.867	1.687	.707±.037	1.192±.033	- .687±.071	- .133±.028
K-5	2.06	.880	1.643	.792±.041	1.301±.036	- .643±.069	- .120±.028
MSV1 section (figure 8)							
Upper part							
MSV1-1	1.96	1.027	.910	.599±.031	.545±.015	+ .090±.038	+ .027±.033
MSV1-2	2.23	1.023	1.036	.468±.024	.485±.014	- .036±.044	+ .023±.033
MSV1-3	1.93	1.021	1.056	.626±.033	.661±.018	- .056±.044	+ .021±.033
MSV1-4	2.06	1.031	1.101	.472±.025	.520±.015	- .101±.046	+ .031±.033
MSV1-5	2.91	1.036	.999	.497±.026	.496±.014	+ .001±.042	+ .036±.033
MSV1-6	2.16	1.009	1.170	.531±.028	.621±.017	- .171±.049	+ .009±.032
MSV1-7	2.23	1.023	1.089	.483±.025	.526±.015	- .089±.046	+ .023±.033
Lower part							
MSV1-8	3.36	1.019	.973	.521±.027	.507±.014	+ .023±.041	+ .019±.033
MSV1-9	4.72	1.007	.861	.773±.040	.666±.109	+ .139±.036	+ .007±.032
MSV1-10	4.49	1.017	.816	.760±.040	.620±.017	+ .184±.034	+ .017±.033
MSV1-11	4.44	1.009	.764	.825±.043	.630±.018	+ .236±.032	+ .009±.032
MSV1-12	5.38	1.018	.674	.959±.049	.647±.018	+ .326±.028	+ .018±.033
MSV1-13	5.21	1.015	.780	.753±.039	.588±.016	+ .221±.033	+ .015±.032

Table 2. Isotopic ratios of uranium and thorium required for U-trend plots (cont'd)

Sample	U ppm	Activity Ratios					
		$\frac{^{234}\text{U}}{^{238}\text{U}}$	$\frac{^{230}\text{Th}}{^{238}\text{U}}$	$\frac{^{238}\text{U}}{^{232}\text{Th}}$	$\frac{^{230}\text{Th}}{^{232}\text{Th}}$	$\frac{(^{238}\text{U}-^{230}\text{Th})}{^{238}\text{U}}$	$\frac{(^{234}\text{U}-^{238}\text{U})}{^{238}\text{U}}$
NSV2 unit (figure 9)							
NSV2-1	1.09	1.000	1.067	0.453±.023	0.481±.013	-0.067±.045	+0.000±.032
NSV2-2	1.75	1.014	1.008	.455±.024	.459±.013	- .083±.042	+ .014±.032
NSV2-3	2.42	1.004	1.119	.420±.022	.471±.013	- .119±.047	+ .004±.032
NSV2-4	2.26	1.016	.975	.498±.026	.486±.014	+ .025±.041	+ .016±.032
NSV2-5	2.65	1.001	1.073	.409±.021	.439±.012	- .073±.045	+ .001±.032
NSV2-6	2.69	1.000	1.053	.433±.023	.456±.013	- .053±.044	+ .000±.032
NSV2-7	2.36	1.008	1.084	.457±.024	.496±.014	- .084±.046	+ .008±.032
NSV2-8	2.79	1.019	1.035	.509±.026	.527±.015	- .035±.043	+ .019±.033
NSV2-9	2.21	1.008	1.051	.491±.026	.516±.014	- .051±.044	+ .008±.032
NSV2-10	2.32	1.021	1.022	.491±.026	.502±.014	- .022±.043	+ .021±.033
FD unit (figure 10)							
FD-1	1.29	.907	1.263	.365±.019	.461±.013	- .263±.053	- .093±.029
FD-2	1.40	.905	1.182	.407±.021	.482±.013	- .182±.050	- .095±.029
FD-3	1.61	.942	1.081	.355±.018	.383±.011	- .081±.045	- .058±.030
FD-4	1.59	.950	1.076	.420±.022	.452±.013	- .076±.045	- .050±.030
FD-5	1.65	.950	1.027	.418±.022	.429±.012	- .027±.043	- .050±.030
FD-6	1.69	.950	1.010	.405±.021	.409±.011	- .010±.042	- .050±.030
FD-7	1.58	.964	1.000	.366±.019	.368±.010	- .004±.042	- .036±.031
FD-8	1.58	.965	.974	.370±.019	.360±.010	+ .026±.041	- .035±.031
P78 (figure 11)							
P75-78M	2.68	.987	1.088	.600±.030	.652±.017	- .088±.045	- .013±.030
78N	2.68	.991	1.129	.519±.026	.586±.015	- .129±.046	- .009±.030
780	2.41	.974	1.182	.482±.024	.570±.015	- .182±.048	- .026±.029
78P	2.57	.988	1.164	.511±.026	.605±.016	- .164±.048	- .012±.030
78Q	2.68	.973	1.093	.499±.025	.546±.014	- .093±.045	- .027±.029
P79 unit (figure 12)							
P75-79F	2.78	.988	.987	.690±.036	.681±.019	+ .013±.041	- .012±.032
79G	3.23	.968	.945	.678±.035	.641±.018	+ .055±.040	- .032±.031
79H	3.28	.983	.988	.625±.032	.618±.017	+ .012±.041	- .017±.031
79I	3.72	.971	1.021	.577±.030	.589±.016	- .021±.043	- .029±.031
P183 upper unit (figure 13)							
P78-183-1	2.84	1.012	1.130	.673±.035	.761±.021	- .130±.047	+ .012±.032
183-2	3.05	1.009	1.106	.673±.035	.744±.021	- .106±.046	+ .009±.032
183-3	3.03	1.009	1.118	.677±.035	.757±.021	- .118±.047	+ .009±.032
183-4	3.07	1.003	1.111	.682±.035	.754±.021	- .111±.047	+ .003±.032
183-5	3.11	.987	1.068	.697±.036	.745±.021	- .068±.045	- .013±.030
P183 lower unit (figure 14)							
P78-183-6	2.88	.981	1.172	.630±.033	.739±.021	- .172±.042	- .019±.031
183-7	2.56	.999	1.138	.640±.033	.728±.020	- .138±.048	- .001±.032
183-8	2.70	.972	1.392	.565±.029	.786±.022	- .392±.058	- .038±.031
183-9	2.57	.959	1.402	.555±.029	.778±.022	- .402±.059	- .041±.031
183-10	2.57	.956	1.350	.590±.031	.797±.022	- .350±.057	- .044±.031
183-11	2.04	.947	1.292	.557±.029	.719±.020	- .292±.054	- .053±.030
183-12	2.72	.940	1.010	.444±.023	.448±.013	- .010±.042	- .060±.030

Table 2. Isotopic ratios of uranium and thorium required for U-trend plots (cont'd)

Sample	U ppm	Activity Ratios					
		$\frac{^{234}\text{U}}{^{238}\text{U}}$	$\frac{^{230}\text{Th}}{^{238}\text{U}}$	$\frac{^{238}\text{U}}{^{232}\text{Th}}$	$\frac{^{230}\text{Th}}{^{232}\text{Th}}$	$\frac{(^{238}\text{U}-^{230}\text{Th})}{^{238}\text{U}}$	$\frac{(^{234}\text{U}-^{238}\text{U})}{^{238}\text{U}}$
P184 unit (figure 15)							
P78-184-1	3.01	0.986	1.082	0.541±.028	0.585±.016	-0.082±.045	-0.014±.032
184-2	2.90	.963	1.053	.530±.028	.558±.016	-.053±.044	-.037±.031
184-3	2.78	.987	1.147	.479±.025	.549±.015	-.147±.048	-.013±.032
184-4	2.23	.971	1.098	.492±.026	.540±.015	-.098±.046	-.029±.031
185-5	2.91	.977	1.086	.449±.023	.488±.014	-.086±.046	-.023±.031
184-6	2.24	.982	1.085	.456±.024	.495±.014	-.085±.046	-.018±.031
184-7	3.23	.984	1.024	.518±.027	.526±.015	-.024±.043	-.016±.032
184-8	2.93	.986	1.063	.456±.024	.489±.014	-.063±.045	-.014±.032
184-9	2.11	.992	1.068	.453±.024	.484±.014	-.068±.045	-.008±.032
Lake Tecopa tuff unit (figure 16)							
T5 E	5.97	1.268	1.059	.855±.044	.906±.025	-.059±.044	+ .268±.041
T5 D	5.33	1.203	1.221	.757±.039	.924±.026	-.221±.051	+ .203±.038
T5 C	5.49	1.179	1.164	.883±.046	1.027±.028	-.164±.049	+ .179±.038
T5 B	4.85	1.012	1.100	.689±.036	.758±.021	-.110±.047	+ .012±.032
T5 A	3.40	1.551	2.153	1.391±.072	2.996±.084	-1.153±.090	+ .551±.050
T6 E	4.80	1.290	1.538	.873±.045	1.343±.038	-.538±.065	+ .290±.041
T6 D	5.90	1.287	1.333	.988±.051	1.317±.037	-.333±.056	+ .287±.041
T6 C	5.92	1.286	1.402	.946±.049	1.326±.037	-.402±.059	+ .286±.041
T6 B	16.2	1.452	1.019	4.524±.235	4.612±.129	-.019±.043	+ .452±.046
T6 A	3.30	1.647	2.264	1.044±.054	2.364±.066	-1.264±.095	+ .647±.053
Lake Tecopa tuff B unit (figure 17)							
T128 D	3.59	1.092	1.242	1.390±.072	1.727±.048	-.242±.052	+ .092±.035
T128 C	6.38	1.008	1.000	1.031±.054	1.031±.029	.000±.042	+ .008±.032
T128 A	1.61	1.090	1.154	1.527±.079	1.762±.049	-.154±.048	+ .090±.035
T148 M	4.26	1.048	1.095	1.033±.054	1.130±.032	-.095±.046	+ .048±.033
Lake Tecopa tuff C unit (figure 18)							
T122 C	2.17	1.053	1.199	.310±.016	.372±.010	-.199±.050	+ .053±.034
T122 B	1.15	1.048	1.109	.379±.016	.421±.012	-.109±.047	+ .048±.033
T122 A	2.87	1.030	1.100	.298±.016	.328±.009	-.100±.046	+ .030±.033
CCA section (figure 19)							
CCA-1	3.32	1.069	1.287	.661±.034	.850±.024	-.287±.054	+ .069±.034
CCA-2	4.95	1.202	.949	.991±.052	.940±.026	+ .051±.040	+ .202±.038
CCA-3	5.64	1.262	.945	.952±.049	.900±.025	+ .055±.040	+ .262±.040
CCA-4	3.95	1.152	1.143	.762±.040	.871±.024	-.143±.048	+ .152±.037
CCA-5	3.59	1.032	1.417	.603±.031	.854±.024	-.417±.060	+ .032±.033
NSV3 upper unit (figure 20)							
NSV3U-1	2.50	1.000	.880	.644±.033	.566±.016	+ .120±.037	+ .000±.032
NSV3U-2	1.95	1.010	1.006	.566±.029	.569±.016	-.006±.042	+ .010±.032
NSV3U-3	3.53	1.004	1.032	.531±.028	.548±.015	-.032±.043	+ .004±.032
NSV3U-4	3.45	1.020	.970	.728±.038	.706±.020	+ .030±.041	+ .020±.033
NSV3U-5	2.75	1.018	1.003	.615±.032	.616±.017	-.003±.042	+ .018±.033
NSV3U-6	1.69	1.009	1.028	.548±.028	.563±.016	-.028±.043	+ .009±.032
NSV3M-1	4.34	1.022	.958	.538±.028	.516±.014	+ .042±.041	+ .022±.033

Table 2. Isotopic ratios of uranium and thorium required for U-trend plots (cont'd)

Sample	U ppm	Activity Ratios					
		$\frac{^{234}\text{U}}{^{238}\text{U}}$	$\frac{^{230}\text{Th}}{^{238}\text{U}}$	$\frac{^{238}\text{U}}{^{232}\text{Th}}$	$\frac{^{230}\text{Th}}{^{232}\text{Th}}$	$\frac{(^{238}\text{U}-^{230}\text{Th})}{^{238}\text{U}}$	$\frac{(^{234}\text{U}-^{238}\text{U})}{^{238}\text{U}}$
NSV3 lower unit (figure 21)							
NSV3M-2	4.99	1.021	0.919	0.617±.032	0.567±.016	+0.081±.038	+0.021±.033
NSV3L-1	3.42	1.017	.954	.553±.029	.527±.016	+ .046±.040	+ .017±.033
NSV3L-2	3.39	1.011	.978	.543±.028	.531±.015	+ .022±.041	+ .011±.032
NSV3L-3	4.63	1.010	1.035	.412±.021	.426±.012	- .035±.043	+ .010±.032
NSV3L-4	2.29	1.018	1.033	.516±.027	.534±.015	- .033±.043	+ .018±.033
NSV3L-5	2.88	1.012	1.031	.851±.044	.877±.025	- .031±.043	+ .012±.032
NSV3L-6	3.32	1.012	.984	.765±.040	.753±.021	+ .016±.041	+ .012±.032
NSV3L-7	6.84	.994	.985	1.677±.087	1.652±.046	+ .015±.041	- .006±.032
NSV3L-8	13.1	.969	1.003	3.263±.170	3.273±.092	- .003±.042	- .031±.031
GF section (figure 22)							
GF-1	1.98	.935	1.332	.450±.023	.599±.017	- .332±.056	- .065±.030
GF-2	1.93	.946	1.340	.413±.021	.553±.015	- .340±.056	- .054±.030
GF-3	2.03	.890	1.316	.421±.022	.555±.015	- .316±.055	- .110±.028
GF-4	1.97	.916	1.320	.416±.022	.549±.015	- .320±.055	- .084±.029
GF-5	1.86	.942	1.333	.416±.022	.554±.015	- .333±.056	- .058±.030
GF-6	2.50	.979	1.179	.520±.027	.613±.017	- .179±.050	- .021±.032
GF-7	2.10	1.056	1.280	.437±.023	.551±.015	- .280±.054	+ .056±.034
GF-8	2.58	1.053	1.110	.217±.011	.241±.007	- .110±.047	+ .053±.034
GF-9	2.07	1.029	1.240	.443±.023	.549±.015	- .240±.052	+ .029±.033
76G27	7.31	1.008	.967	.737±.038	.706±.020	+ .033±.041	+ .008±.032

Table 3. U-trend model parameters and ages of deposition units (C indicates calibration unit)

Unit	Description of deposit	U-trend slope	X-intercept	Half period of F(0) (Ka)	U-trend Age (Ka)
1c	PC unit, Piney Creek alluvium, Kassler quadrangle, CO.	+0.045	-2.74	68	5 ± 20
2c	WF unit, late Wisconsin loess, Wabasha County, MN.	+ .050	+1.43	70	7 ± 5
3c	FF unit, late Wisconsin loess, Fillmore County, MN.	+ .082	+ .671	72	12 ± 15
4	K unit, late Wisconsin till, Mower County, MN.	+ .104	+ .596	76	15 ± 15
5	MSV1 unit, Slope wash and till upper part and till of Pinedale glaciation (lower part) Peaceful Valley, CO.	+ .064	- .430	100	12 ± 14
		+ .047	- .061	620	60 ± 50
6	NSV2 unit, till of Bull Lake glaciation, Allens Park, CO.	+ .134	- .119	550	130 ± 80
7c	FD unit, Outer Bull Lake moraine, Sublette County, WY.	+ .225	- .182	440	160 ± 50
8c	P78 unit, Bull Lake moraine, West Yellowstone, MT.	+ .114	- .009	720	150 ± 100
9c	P183 lower unit, Bull Lake loess, West Yellowstone, MT.	+ .138	- .055	640	160 ± 50
10c	P184 lower unit, Bull Lake moraine, West Yellowstone, MT.	+ .177	+ .031	670	190 ± 90
11c	Tuff A unit, Lake Tecopa, Inyo County, CA	- .482	+ .118	550	600 ± 60
12c	Tuff B unit, Lake Tecopa, Inyo County, CA.	- .386	+ .033	660	740 ± 100
13	Tuff C unit, Lake Tecopa Inyo County, CA.	<- .347	- .109	560	>800
14	CCA unit, alluvium, Shirley Mtns. area, WY.	+ .445	- .470	90	60 ± 12
15	NSV3U unit, pre-Bull Lake till, Allens Park, CO.	+ .240	- .057	640	220 ± 70
16	GF section, upper colluvium, Golden fault zone, CO.	- 2.52	- .358	130	190 ± 60
17	GF section, lower colluvium, Golden fault zone, CO.	- .764	- .205	420	440 ± 90

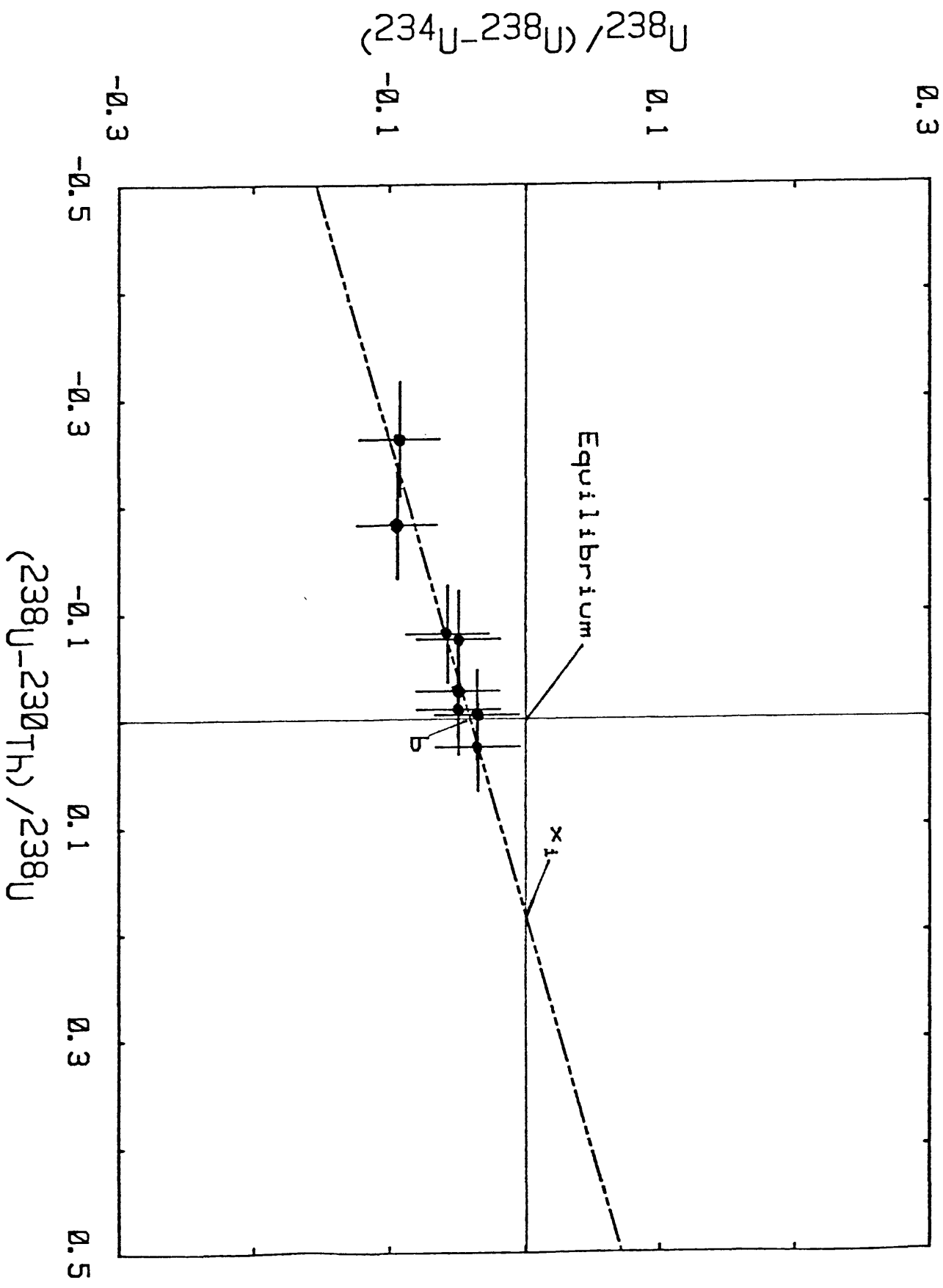


Figure 1. Uranium trend plot of FD unit, Outer Bull Lake Hill, Sublette County, Wyoming. All samples plotted in terms of activity ratios.

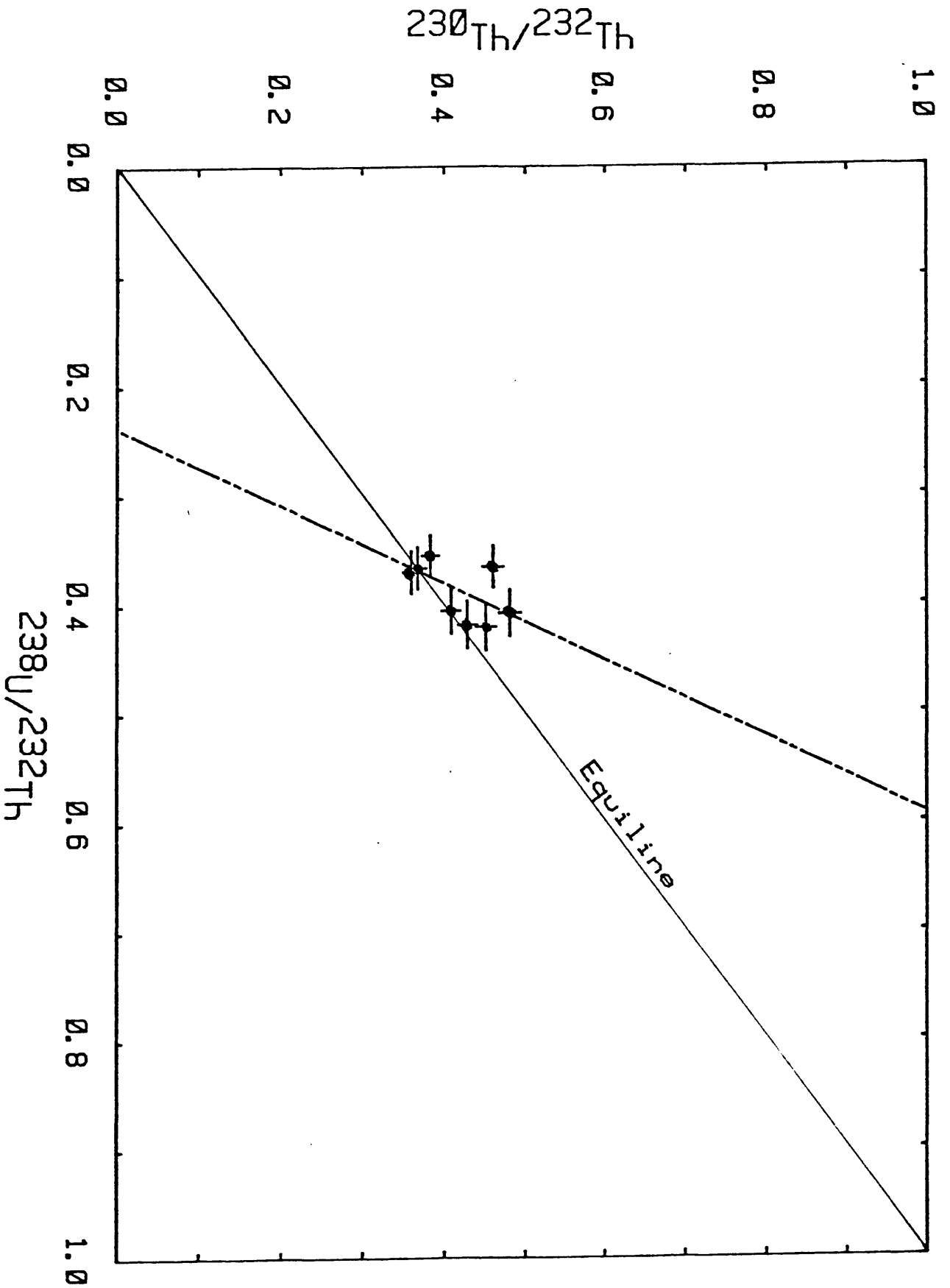


Figure 2. Thorium-Index plot of FD unit, Outer Bull Lake Hill, Sublette County, Wyoming. All samples plotted in terms of activity ratios.

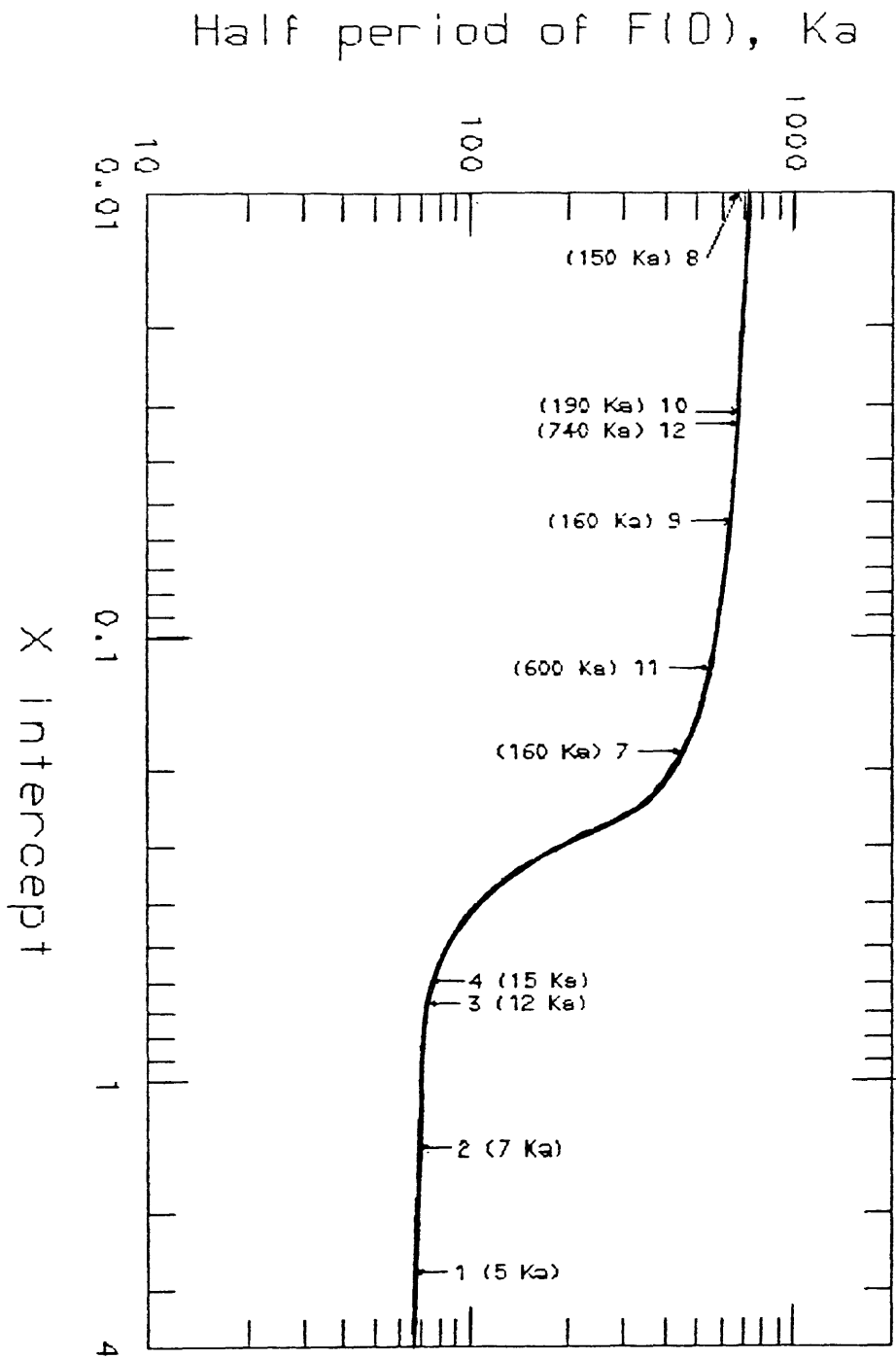


Figure 3. Time-calibration curve for determination of F(O) from X-intercept value. Indices on curve show unit number and uranium-trend age from Table 3.

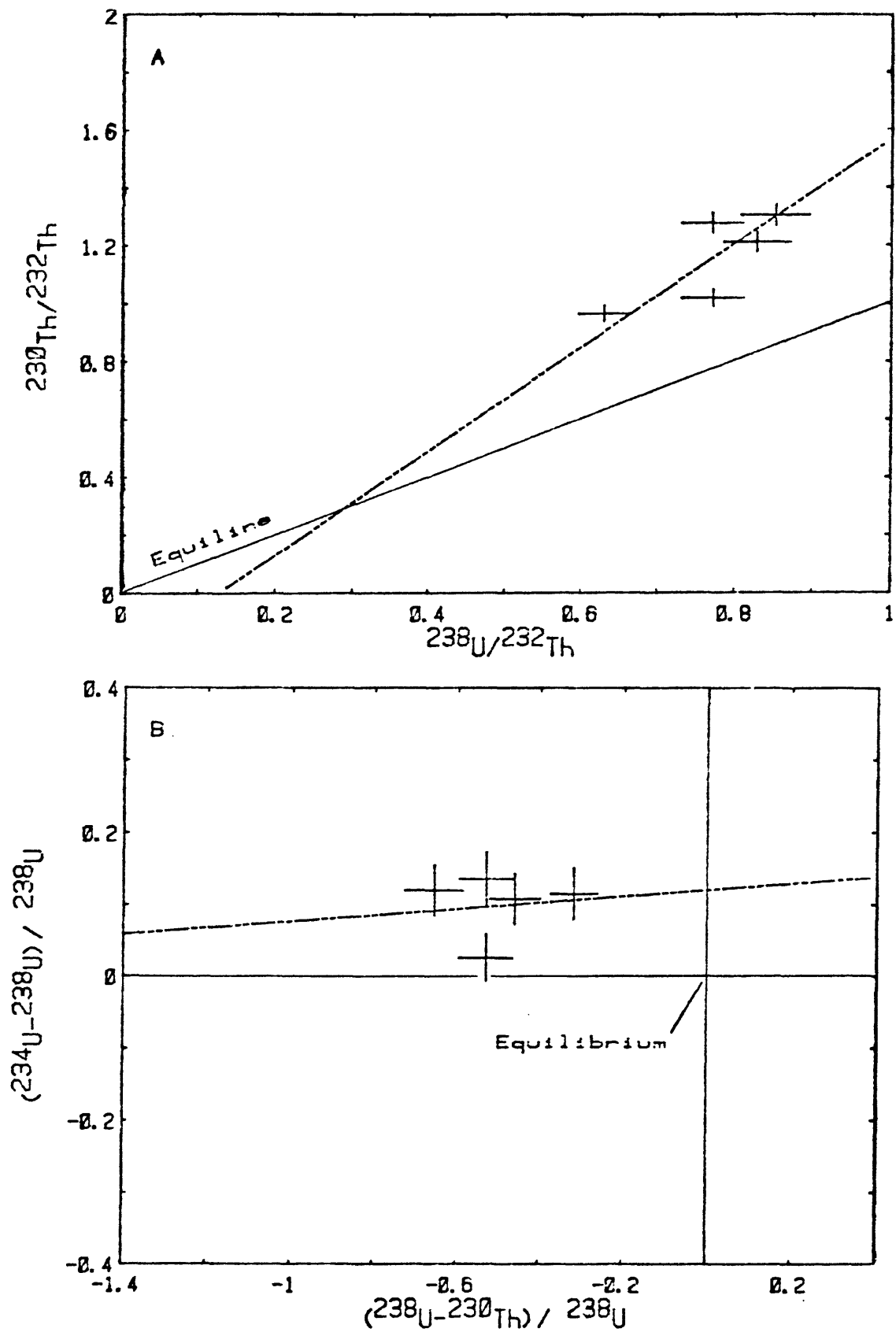


Figure 4. Plots of PC unit, Piney Creek Alluvium, Colorado. A is Th-index, B is U-trend plot.

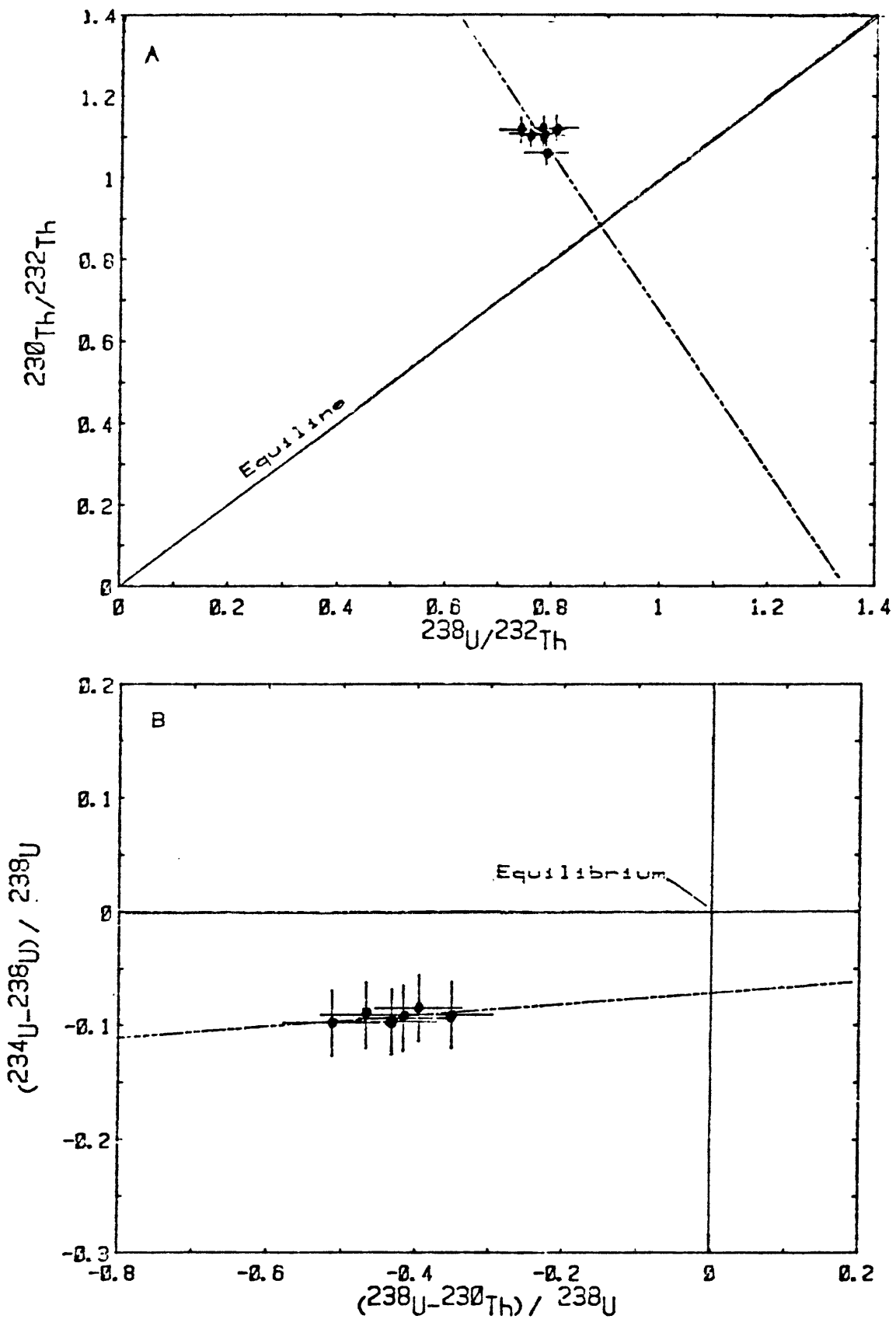


Figure 5. Plots of WF unit, late Wisconsin loess, Minnesota. A is Th-index, B is U-trend plot.

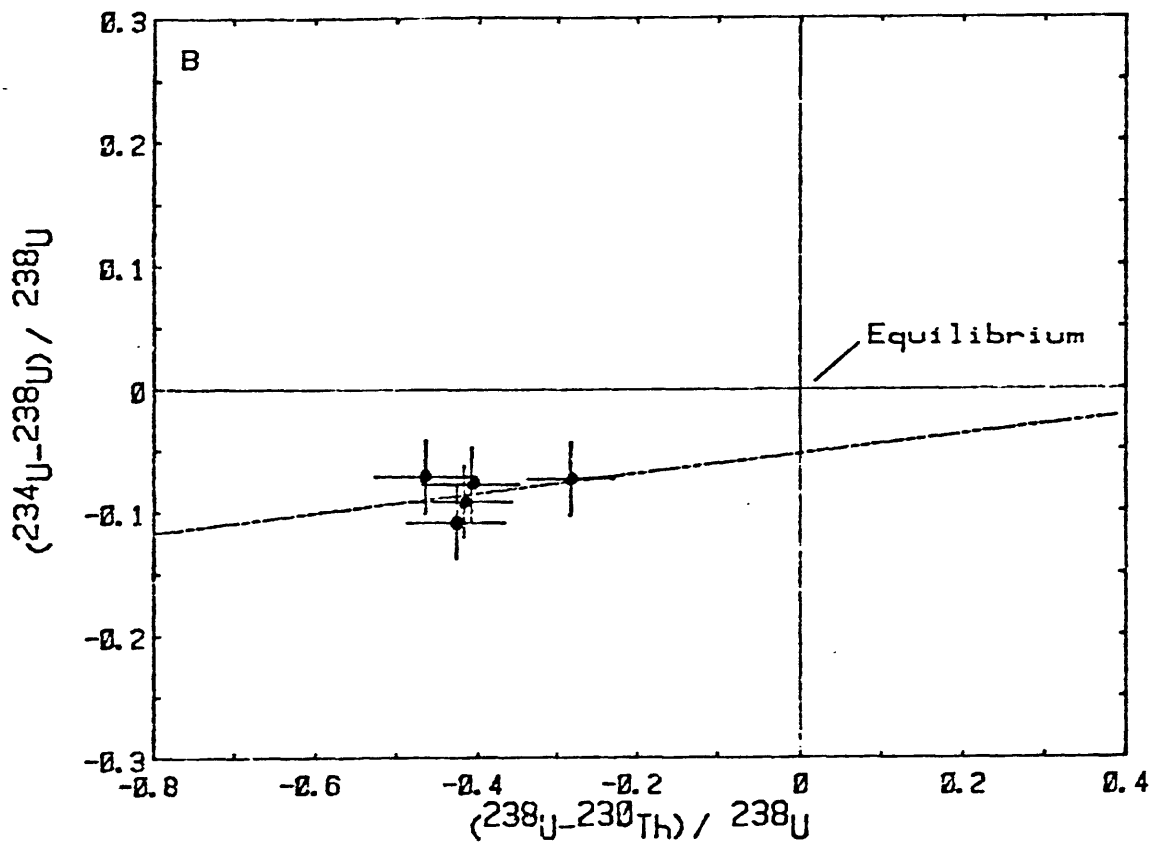
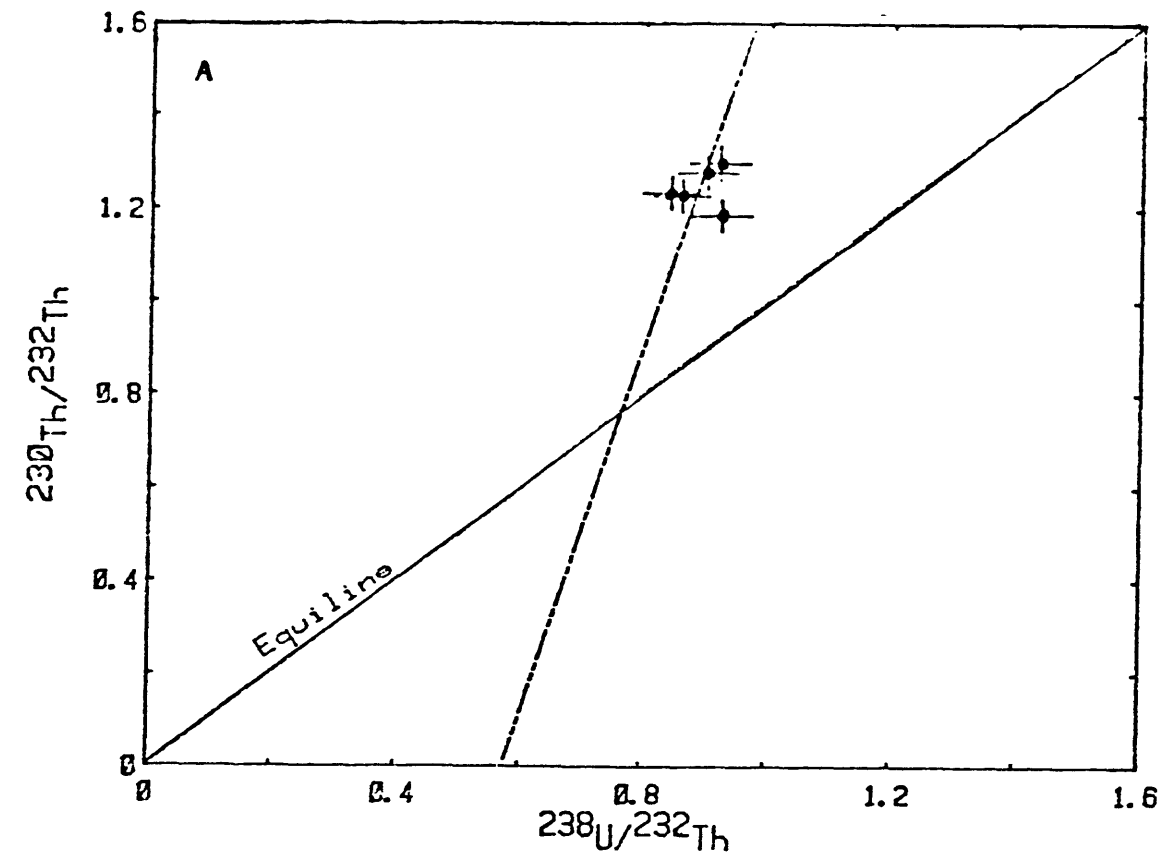


Figure 6. Plots of FF unit, late Wisconsin loess, Minnesota. A is Th-index, B is U-trend plot.

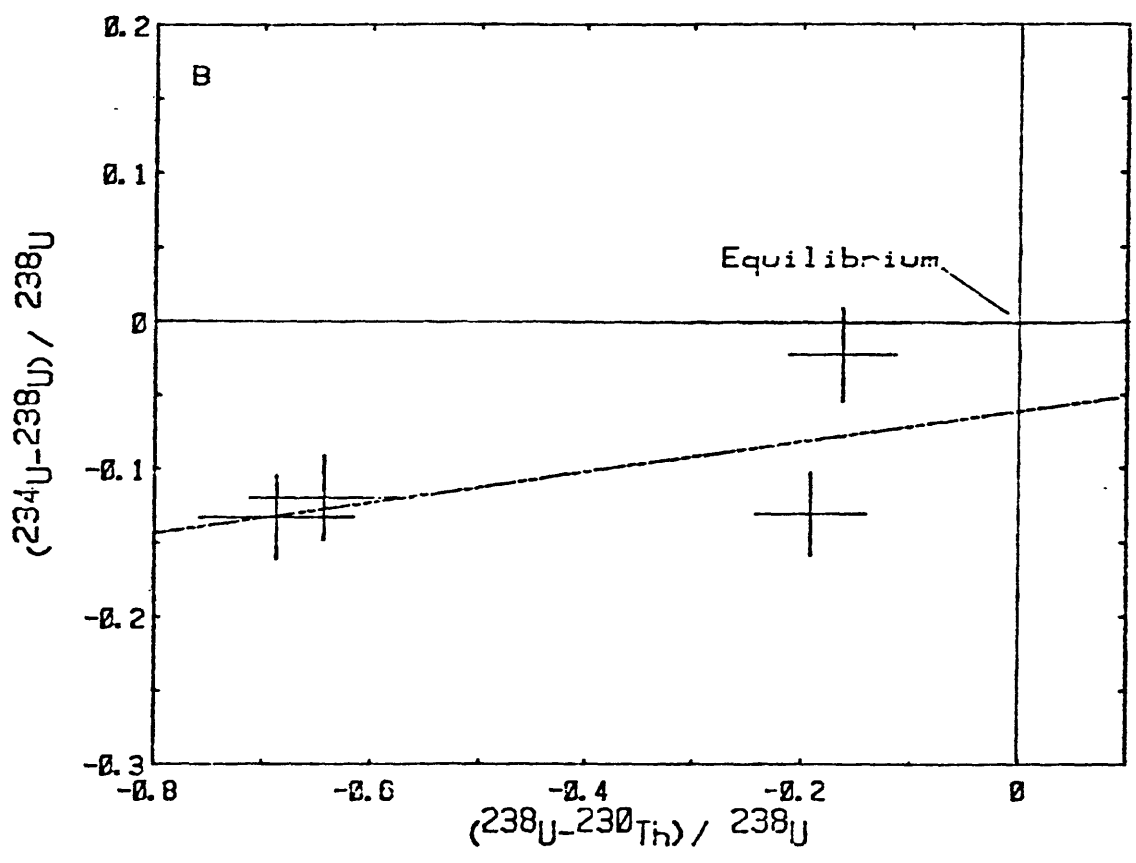
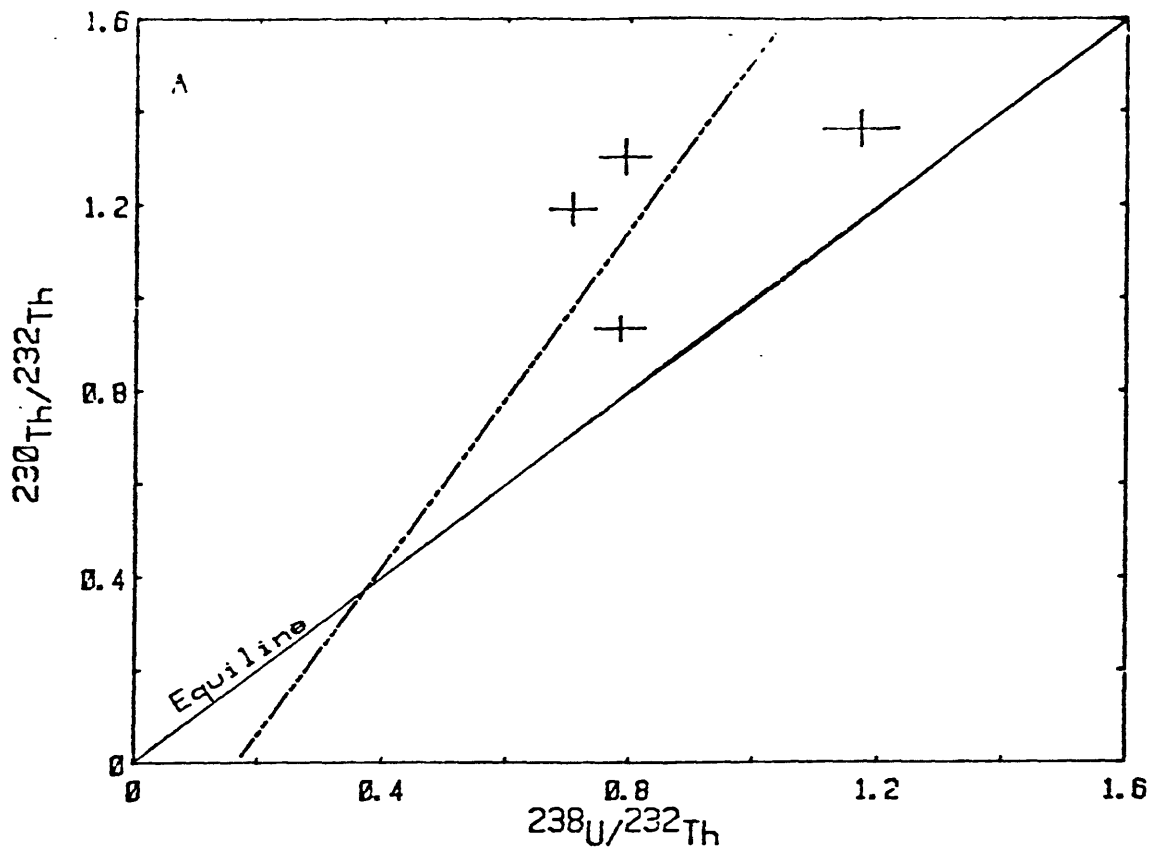


Figure 7. Plots of K unit, Wisconsin till, Minnesota. A is Th-index, B is U-trend plot.

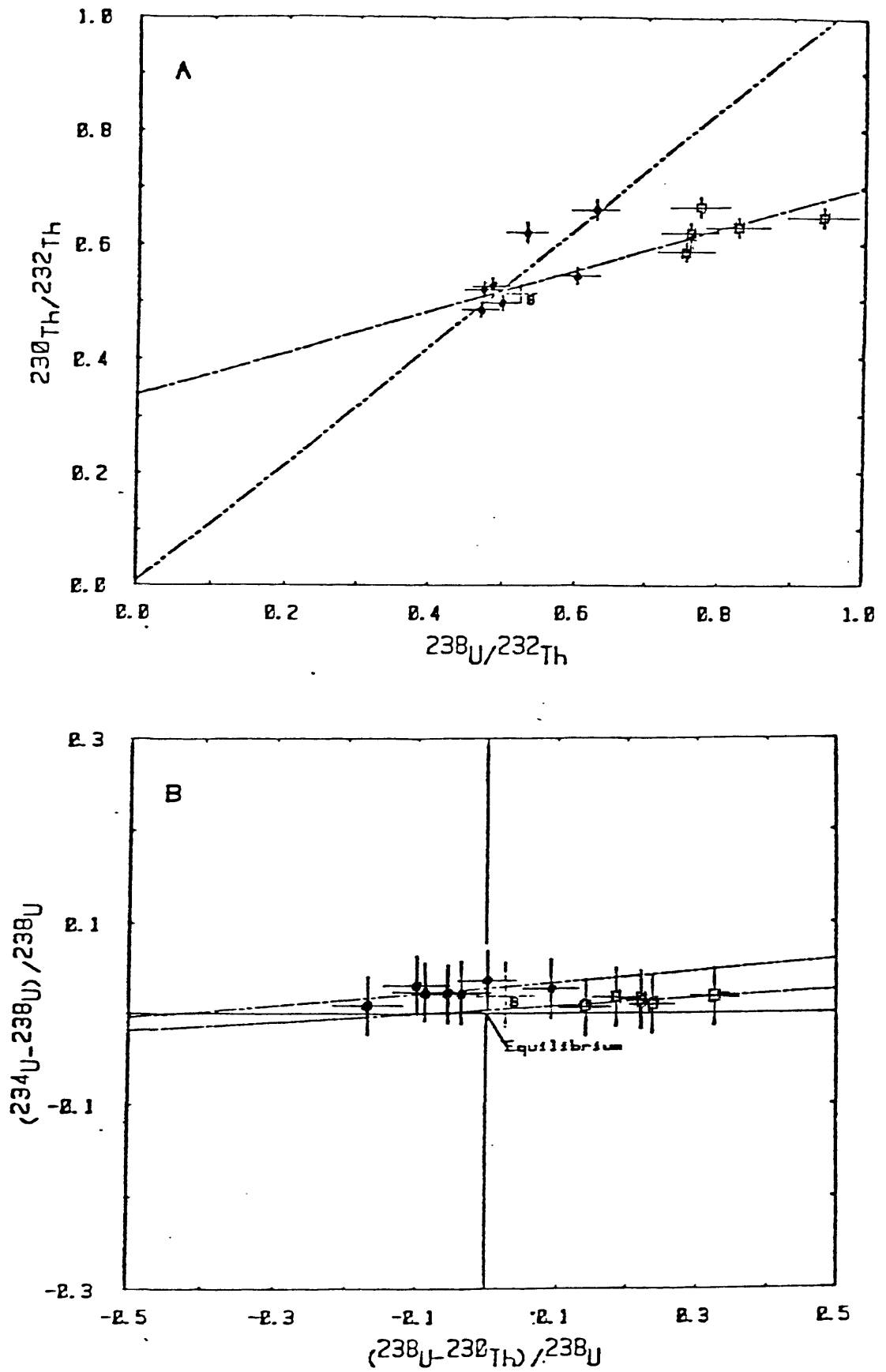


Figure 8. Plots of MSV1 section, Post-Pinedale slopewash and till of Pinedale glaciation, Boulder County, Colorado. A is Th-index, B is U-trend plot.

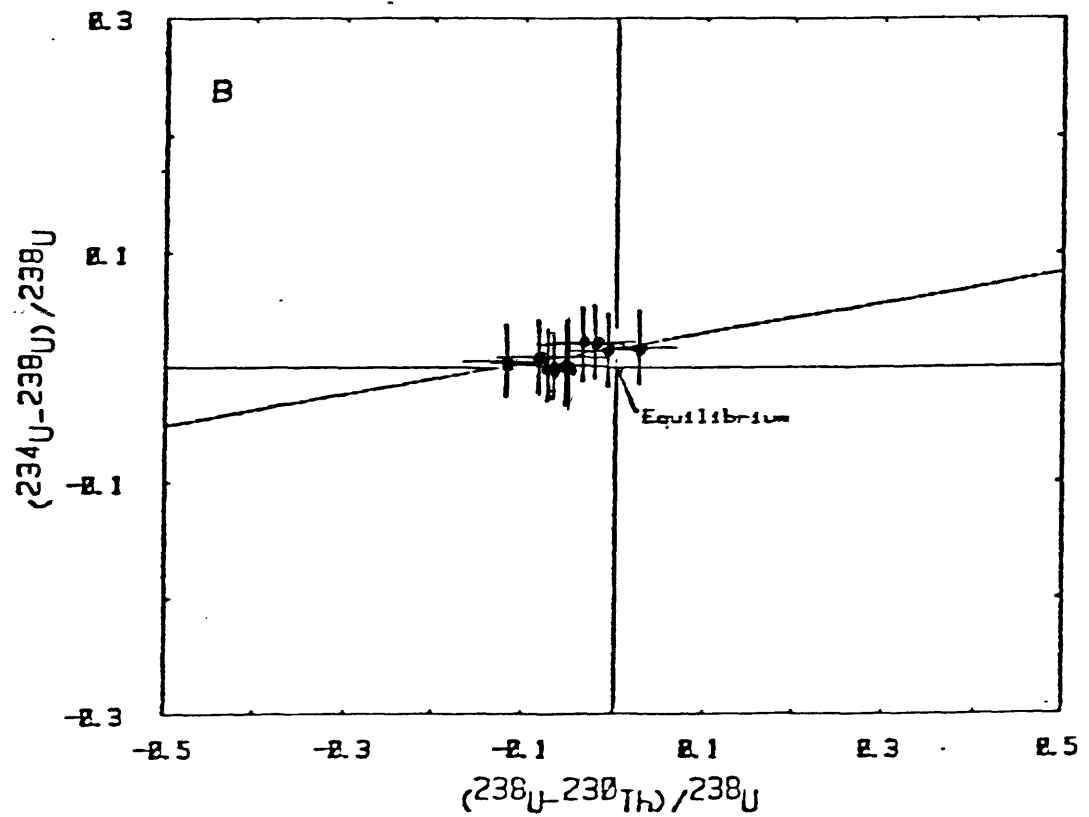
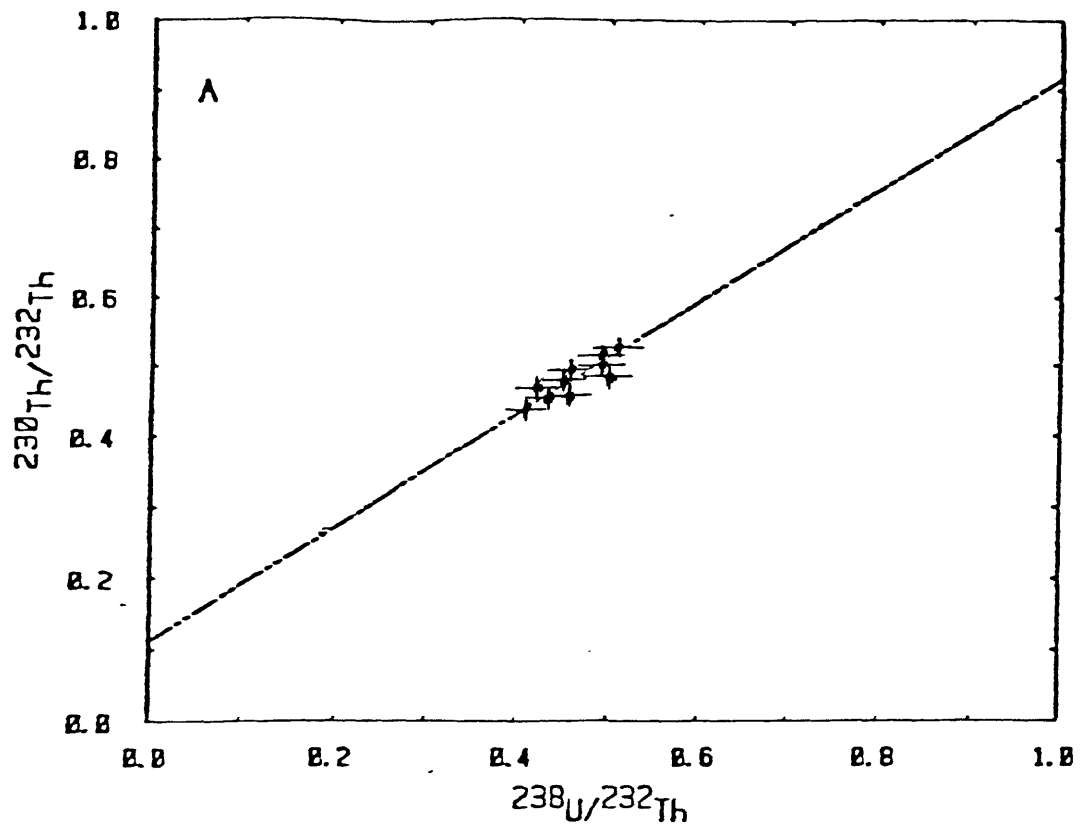


Figure 9. Plots of NSV2 section, till of Bull Lake glaciation, Boulder County, Colorado. A is Th-index, B is U-trend plot.

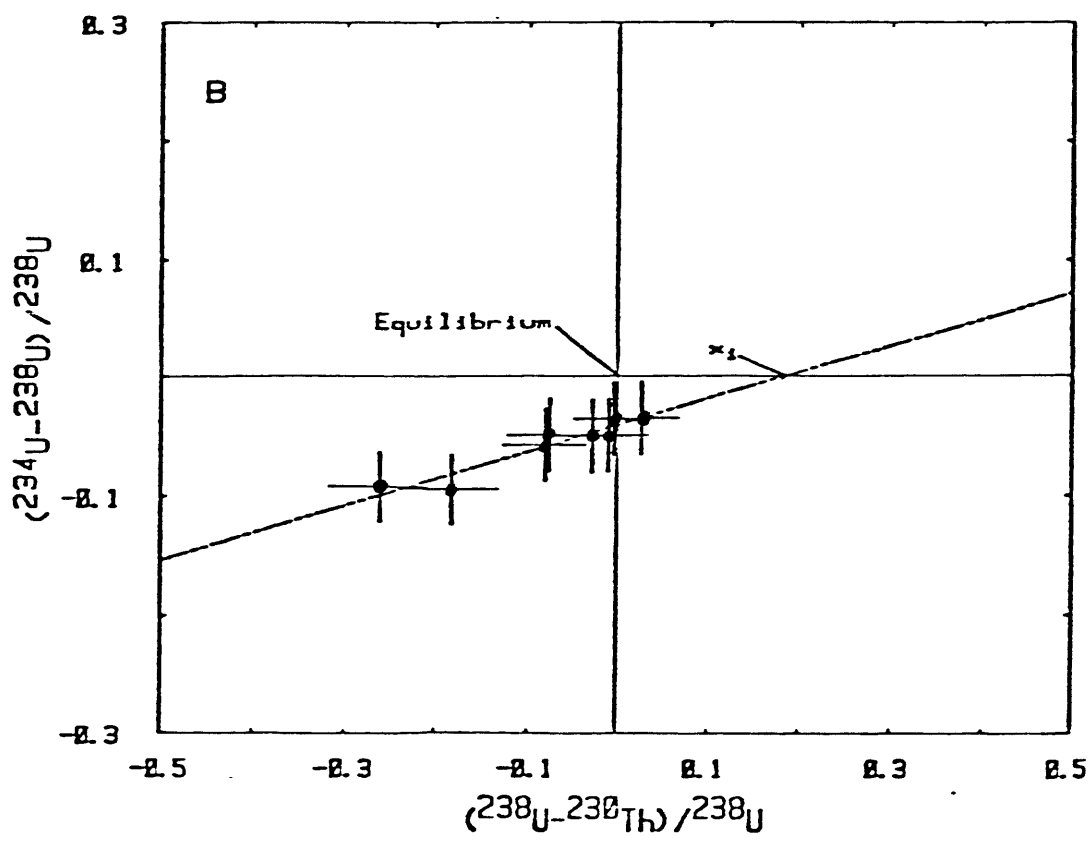
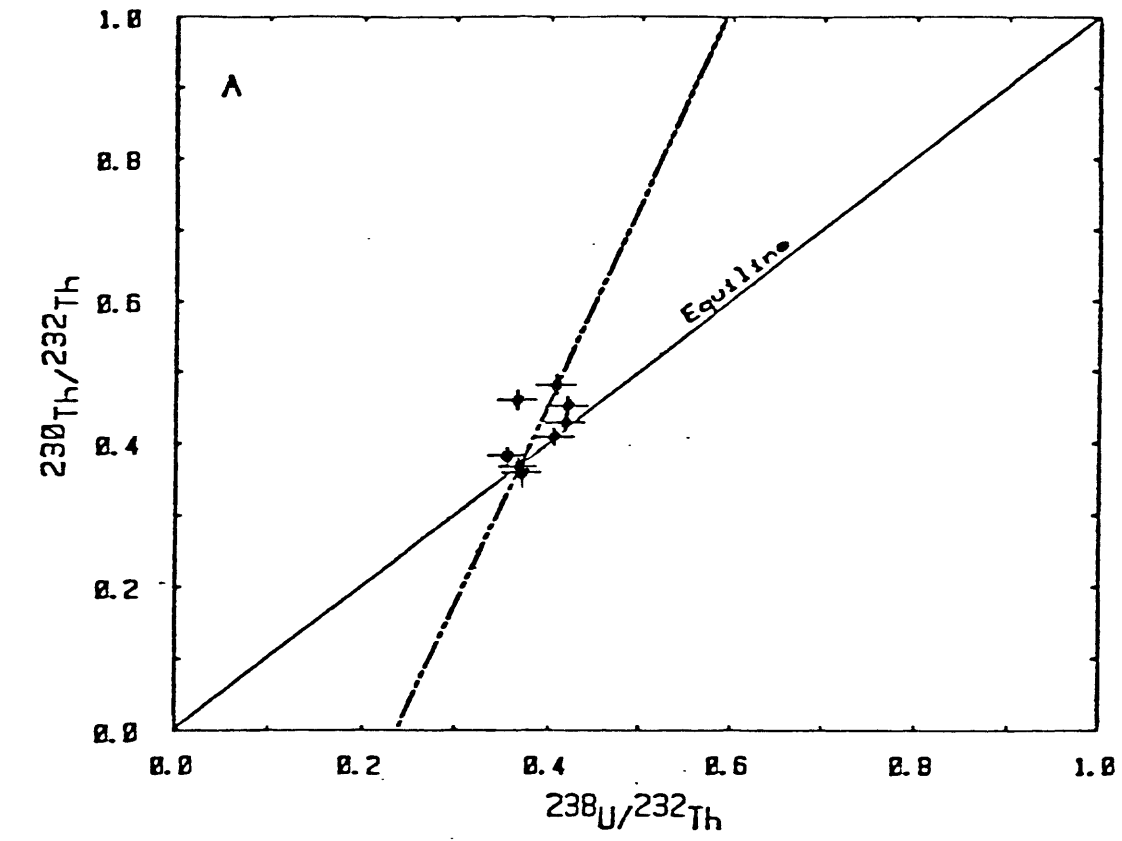


Figure 10. Plots of FD unit, Outer Bull Lake moraine, Sublette County, Wyoming. A is Th-index, B is U-trend plot.

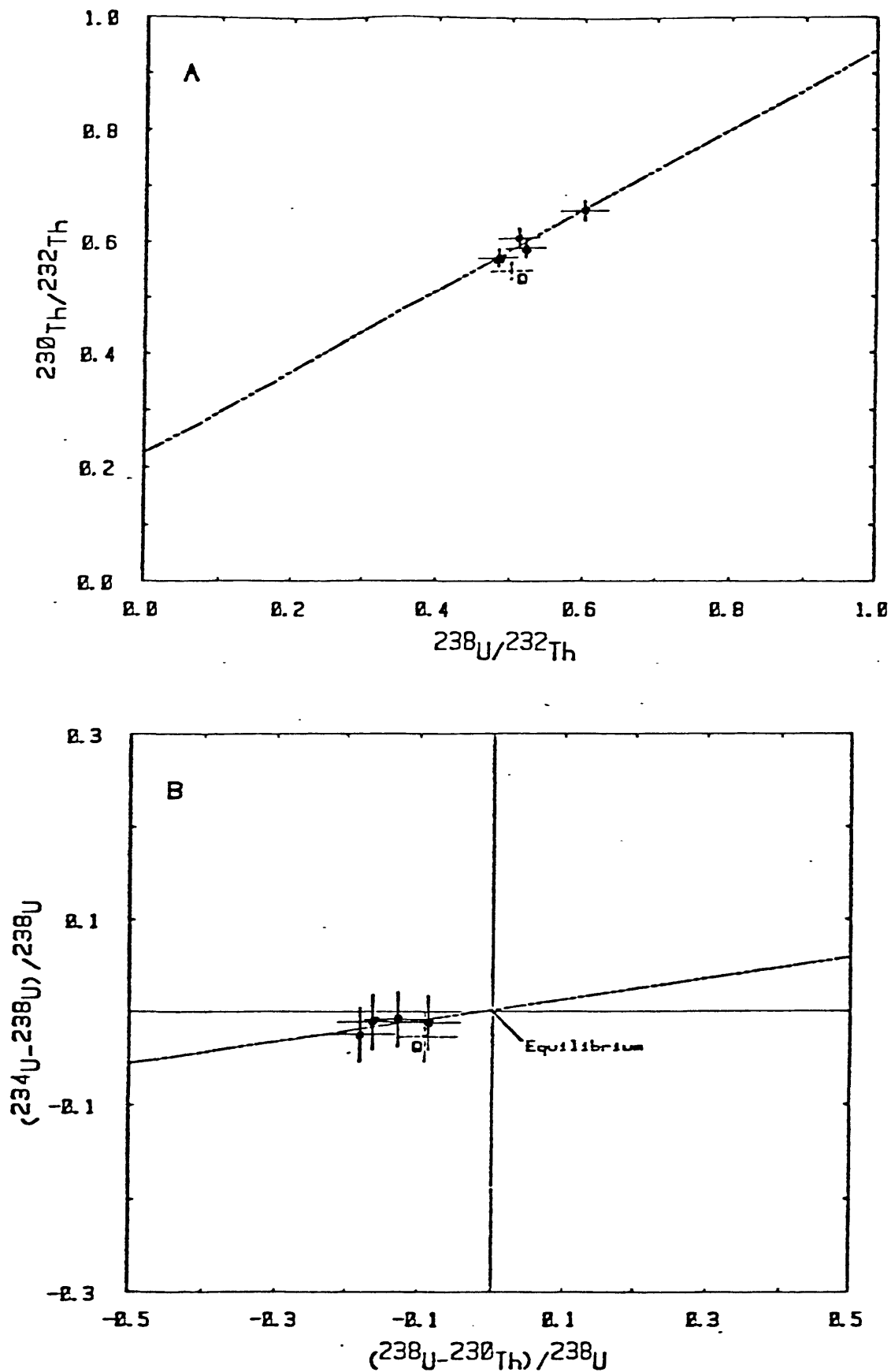


Figure 11. Plots of P78 unit, Bull Lake end moraine, West Yellowstone, Montana. A is Th-index, B is U-trend plot. Sample Q is not included in slope calculation.

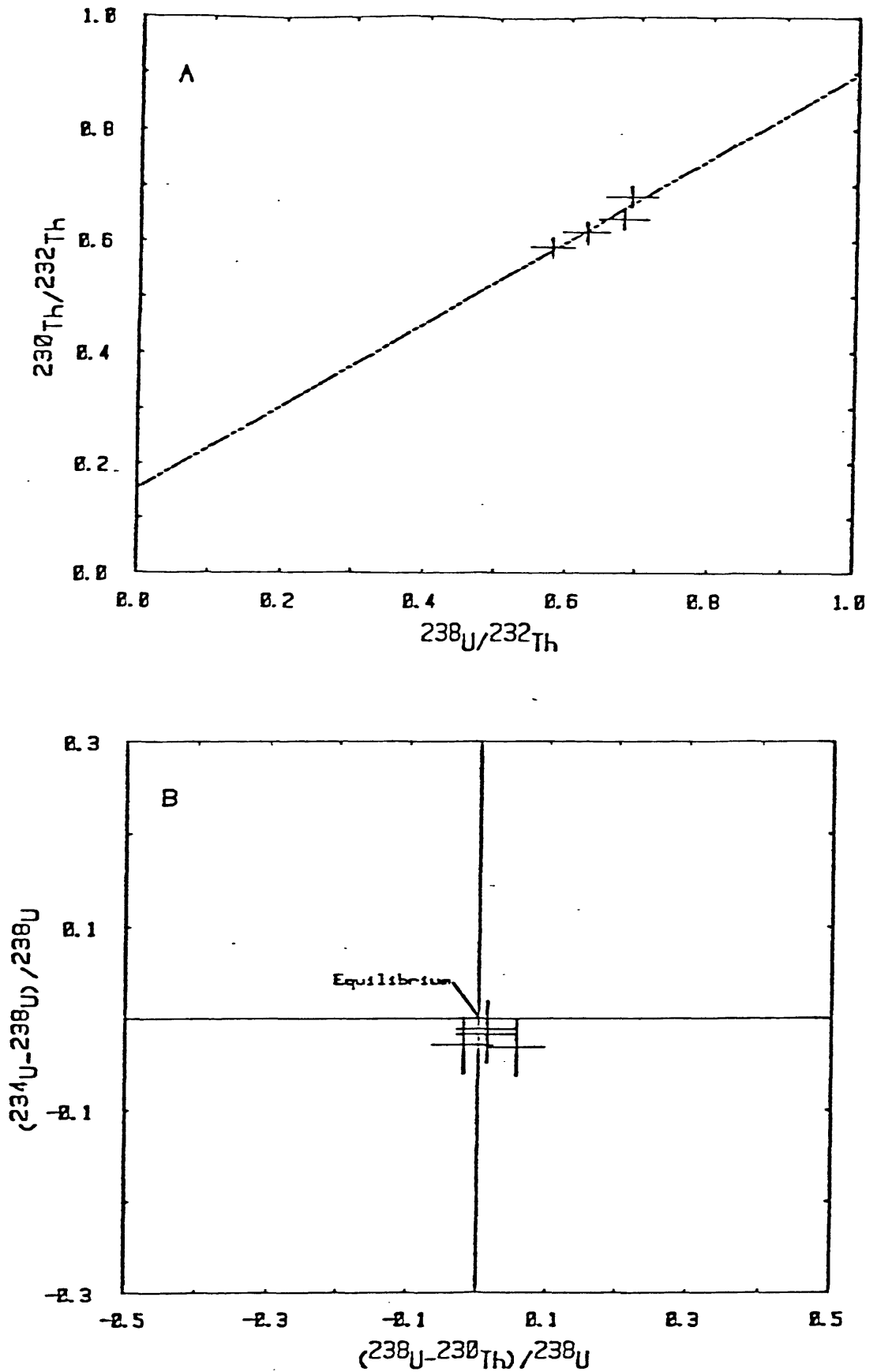


Figure 12. Plots of P79 unit, Pinedale end moraine, West Yellowstone, Montana. A is Th-index, B is U-trend plot; points for U trend have insufficient spread for age calculation.

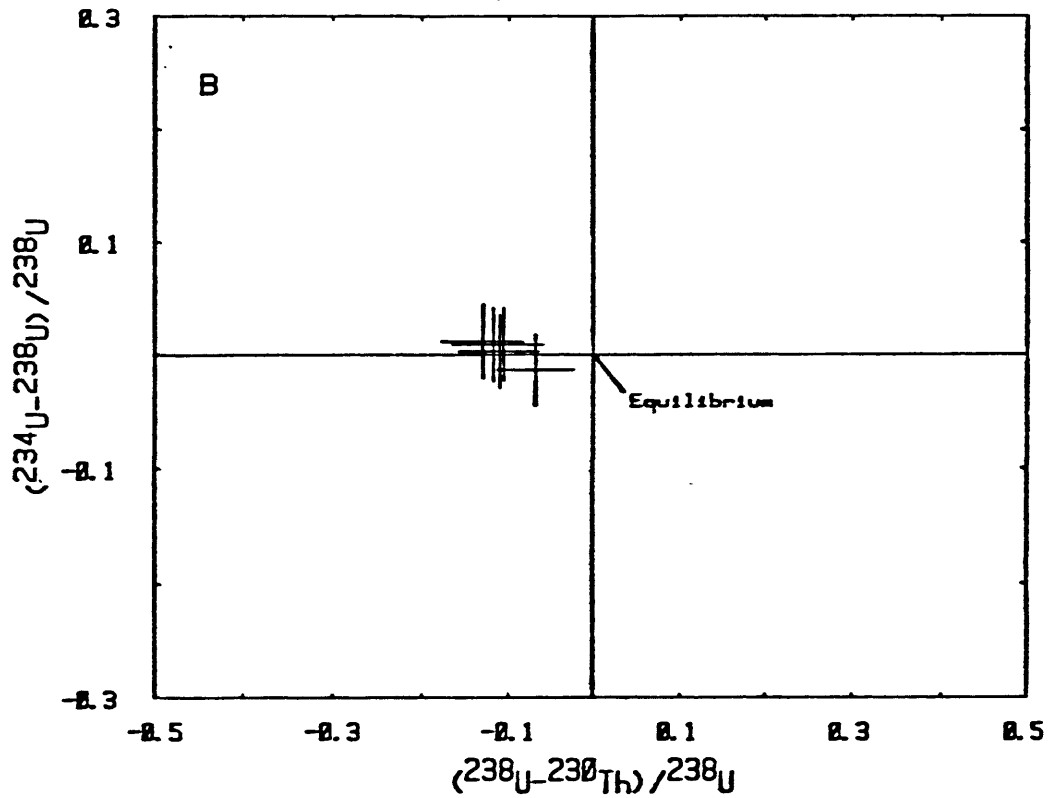
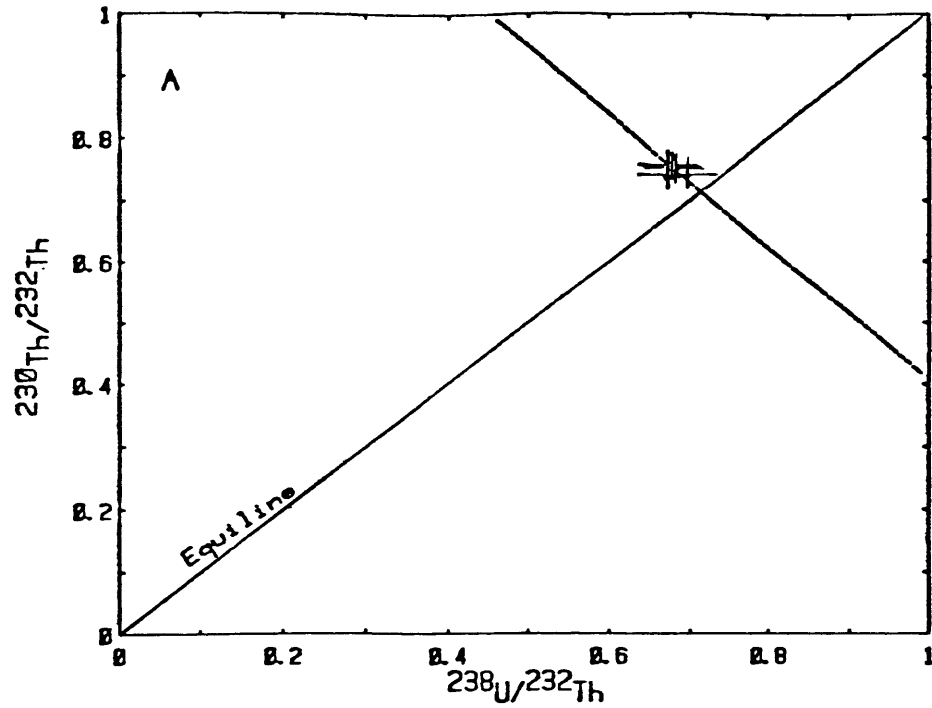


Figure 13. Plots of P183 section, Pinedale loess, West Yellowstone, Montana. A is Th-index, B is U-trend plot; points for U trend have insufficient spread for reliable age calculation.

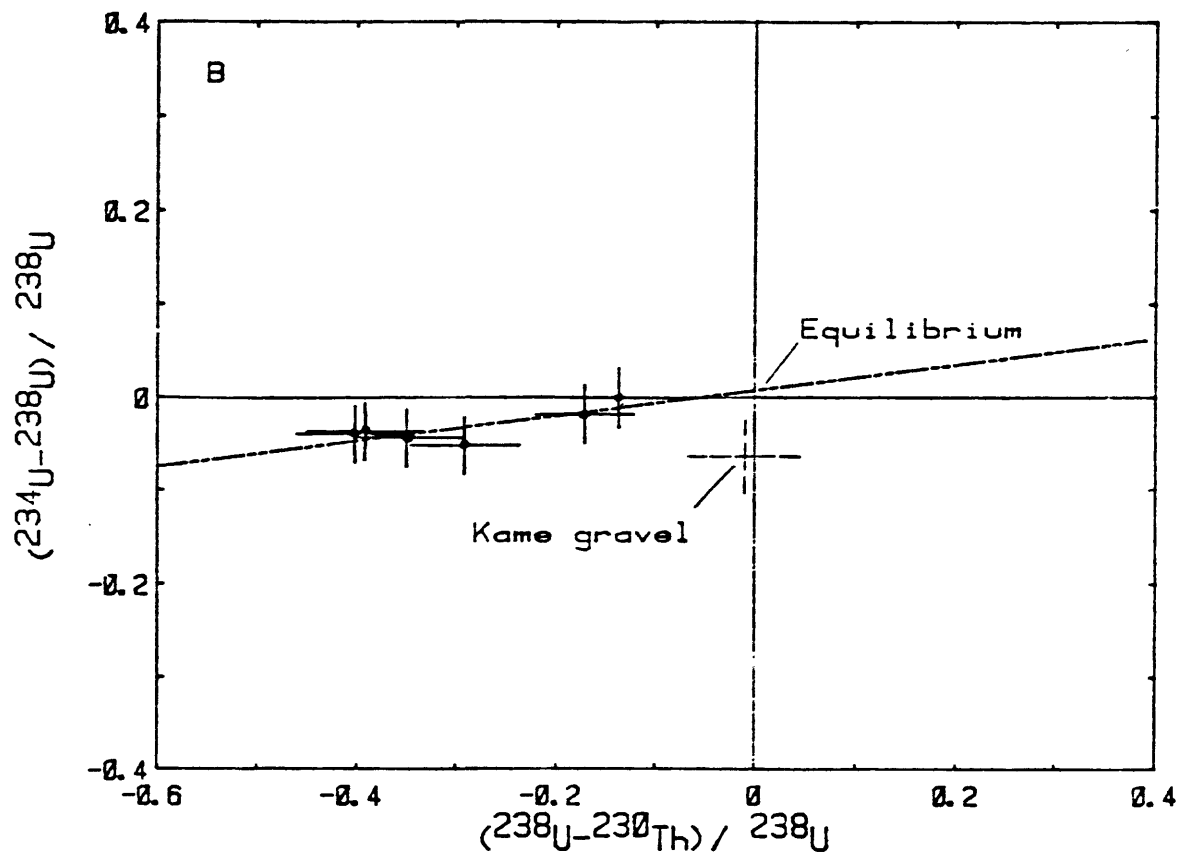
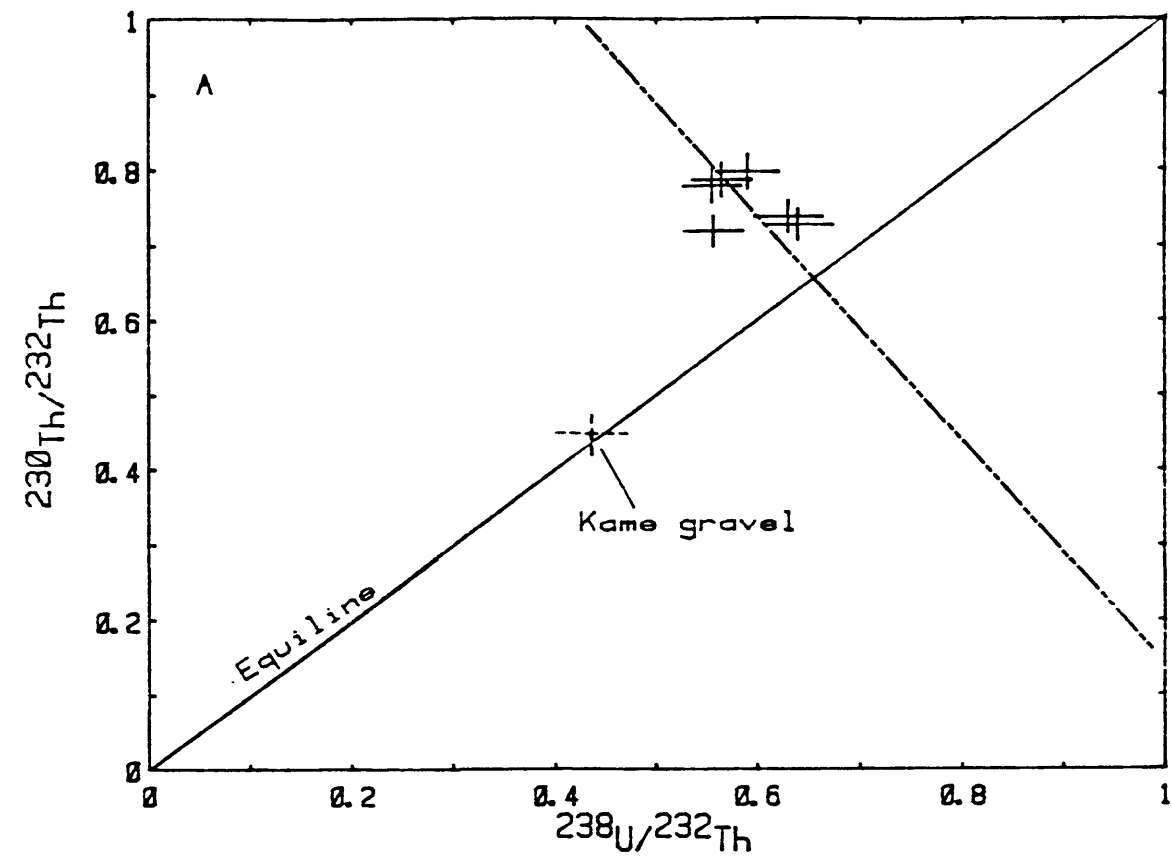


Figure 14. Plots of P183 lower unit, Bull Lake loess, West Yellowstone, Wyoming. A is Th-index, B is U-trend plot. Kame gravel sample is not included in slope calculation.

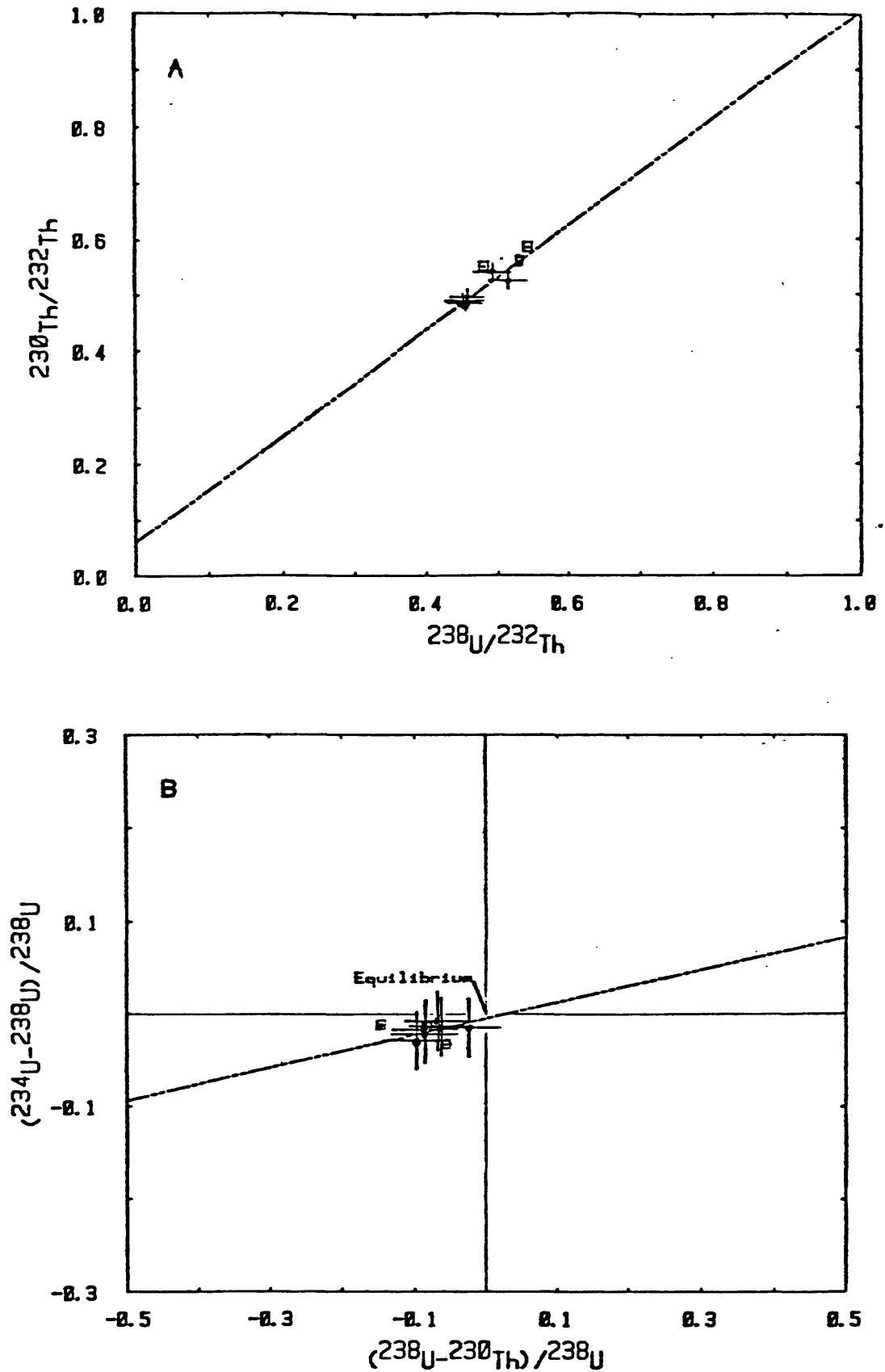


Figure 15. Plots of P184 unit, Bull Lake moraine, West Yellowstone, Montana. A is Th-index, B is U-trend plot; only 6 lower samples (●) containing secondary silica soil horizons are included in slope calculation. The 3 upper samples are indicated by □.

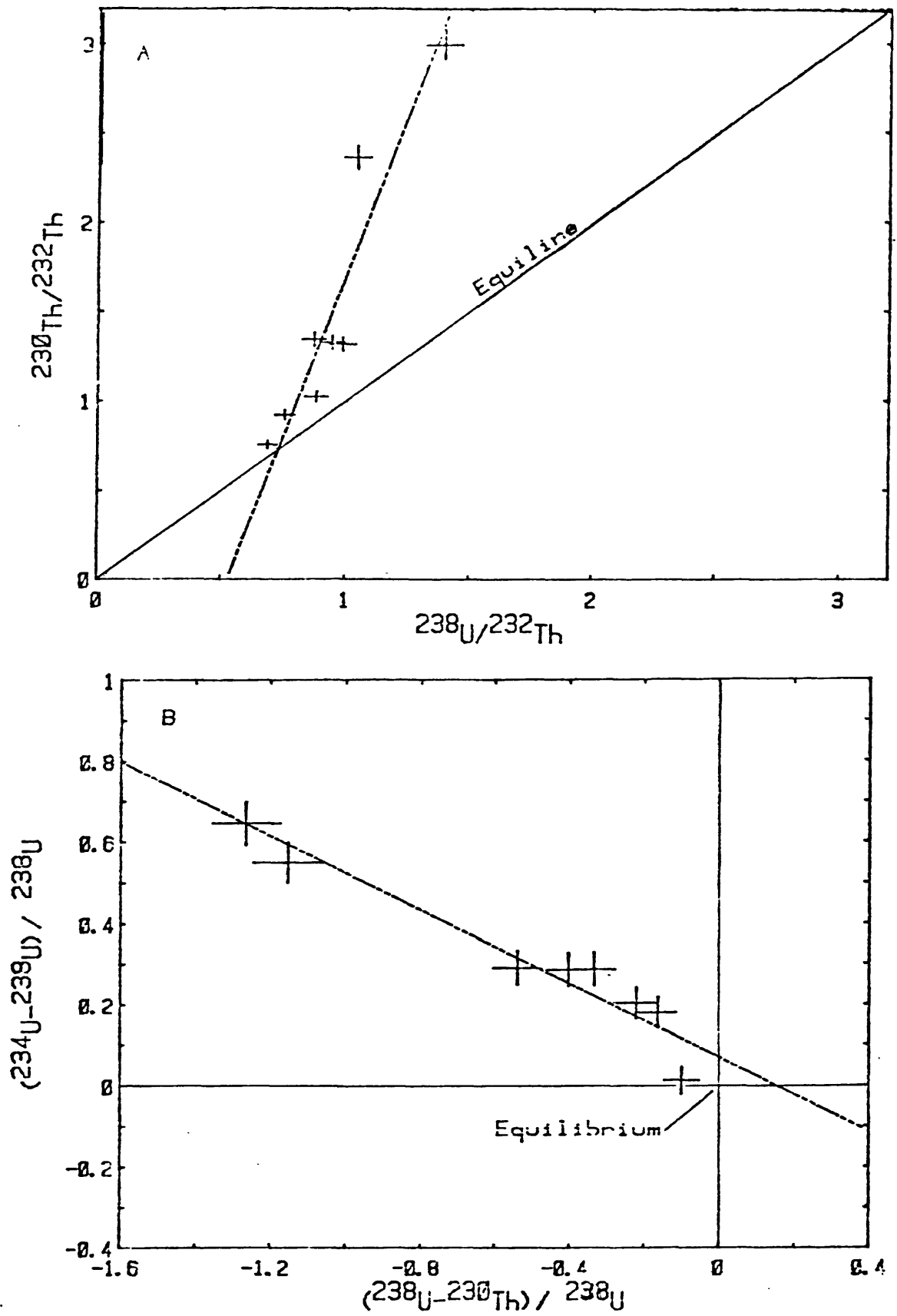


Figure 16. Plots of tuff A unit, Lake Tecopa, California. A is Th-index, B is U-trend plot.

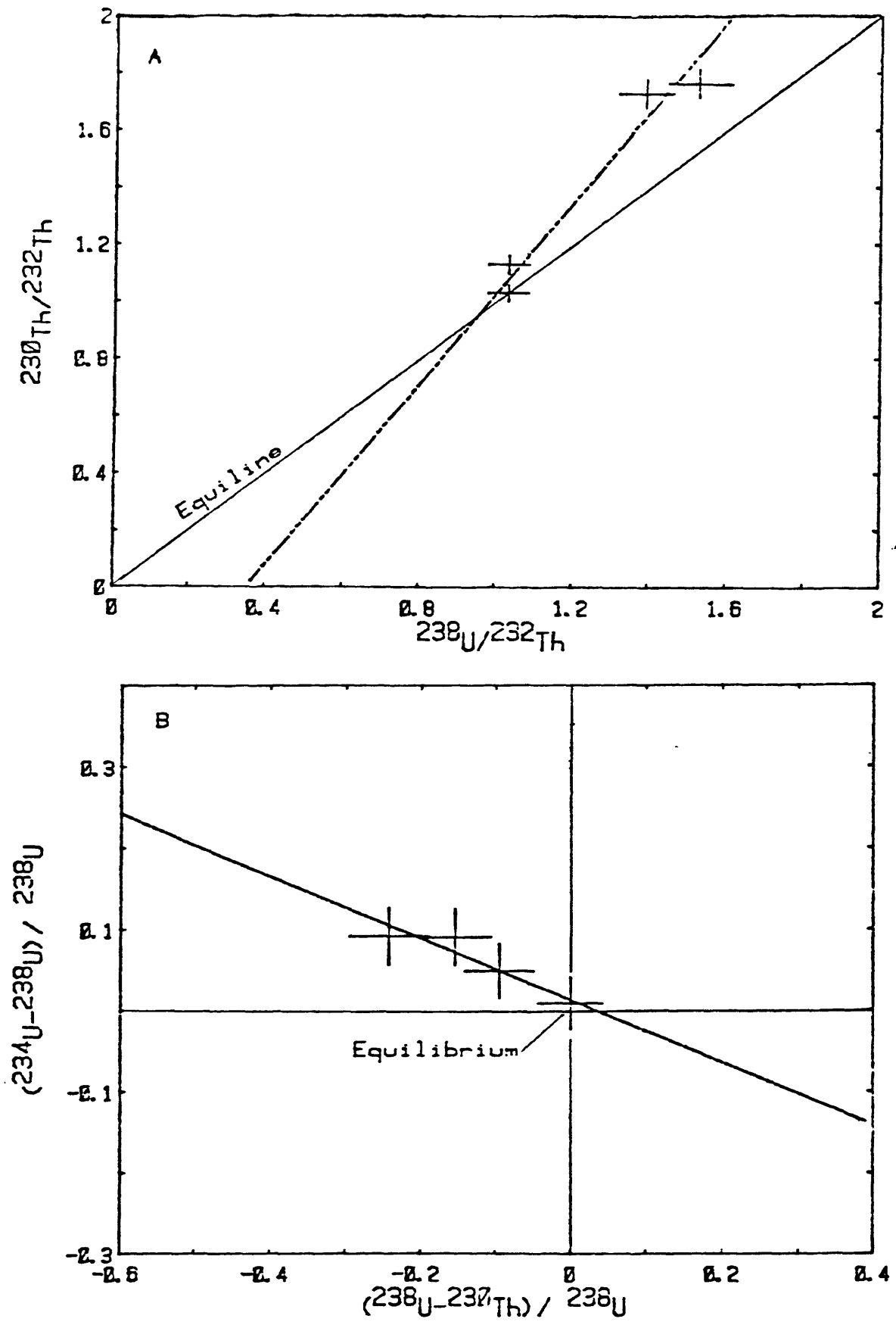


Figure 17. Plots of tuff B unit, Lake Tecopa California. A is Th-index, B is U-trend plot.

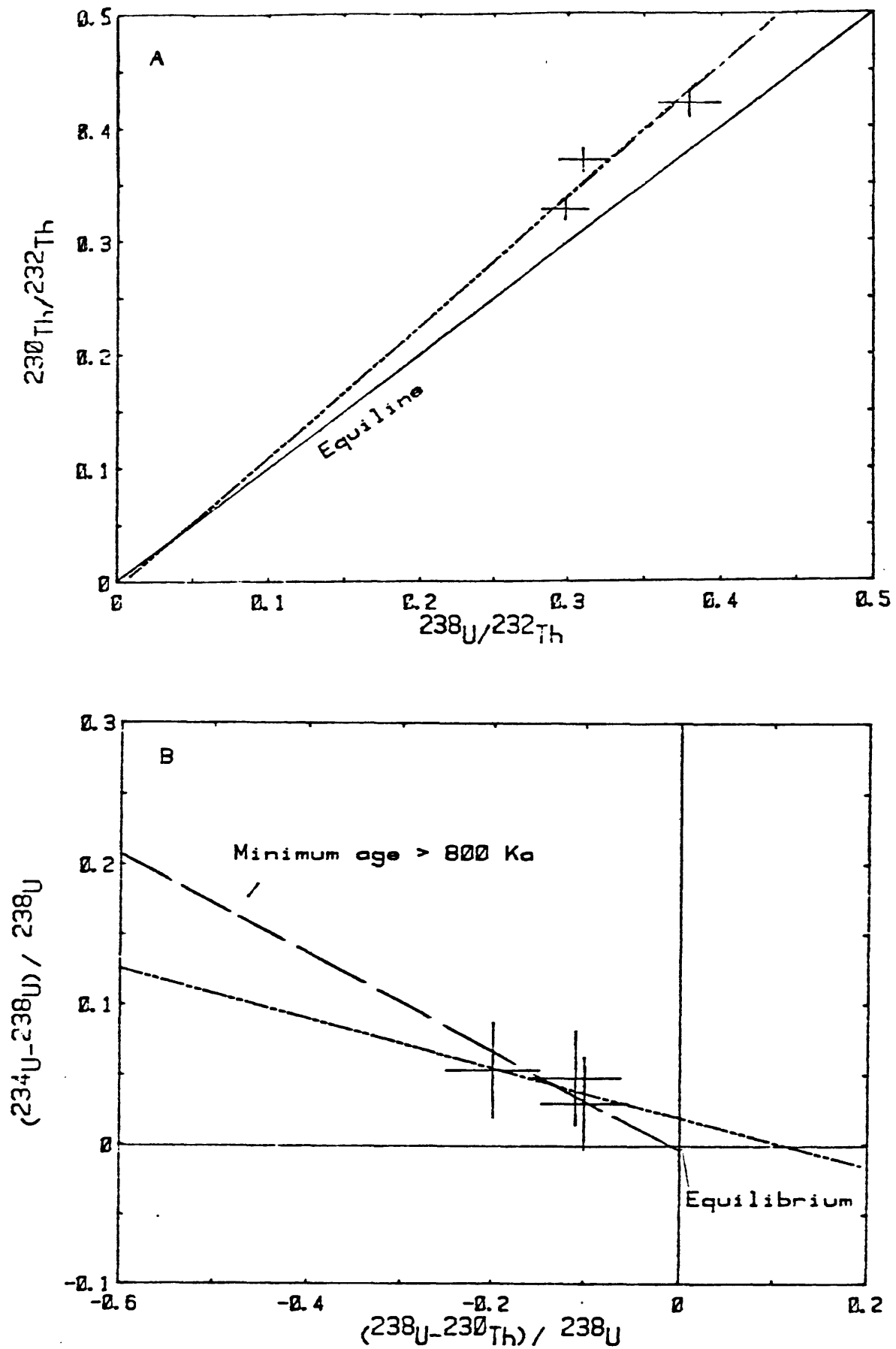


Figure 18. Plots of tuff C unit, Lake Tecopa, California. A is Th-index, B is U-trend plot.

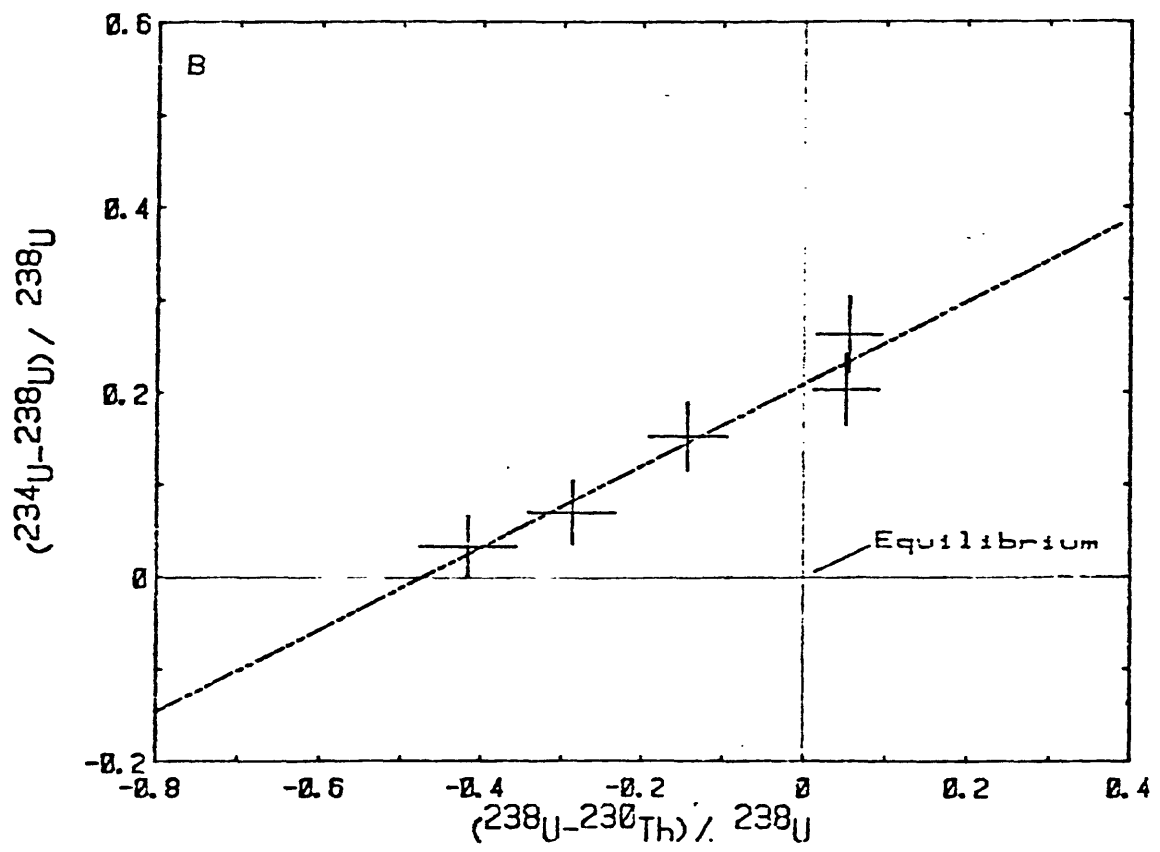
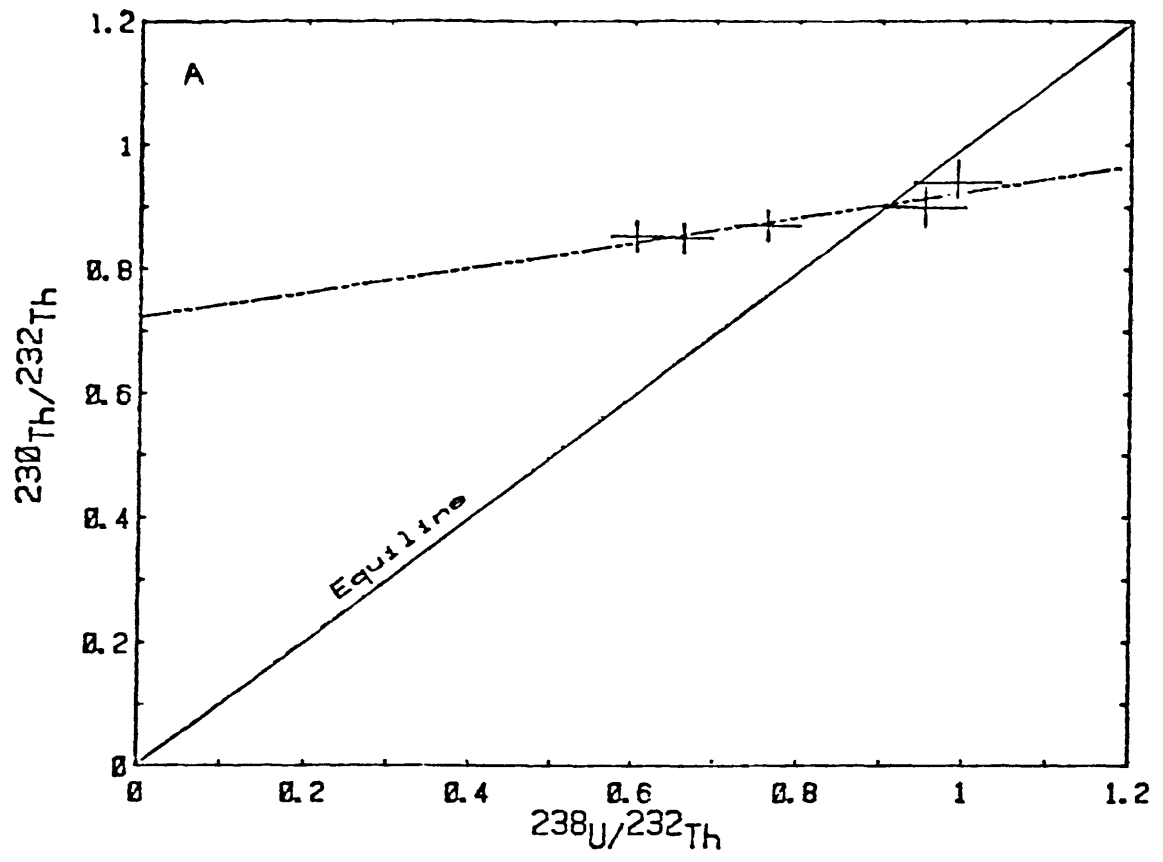


Figure 19. Plots of CCA section of alluvium, Shirley Mountains area, Wyoming. A is Th-index, B is U-trend plot.

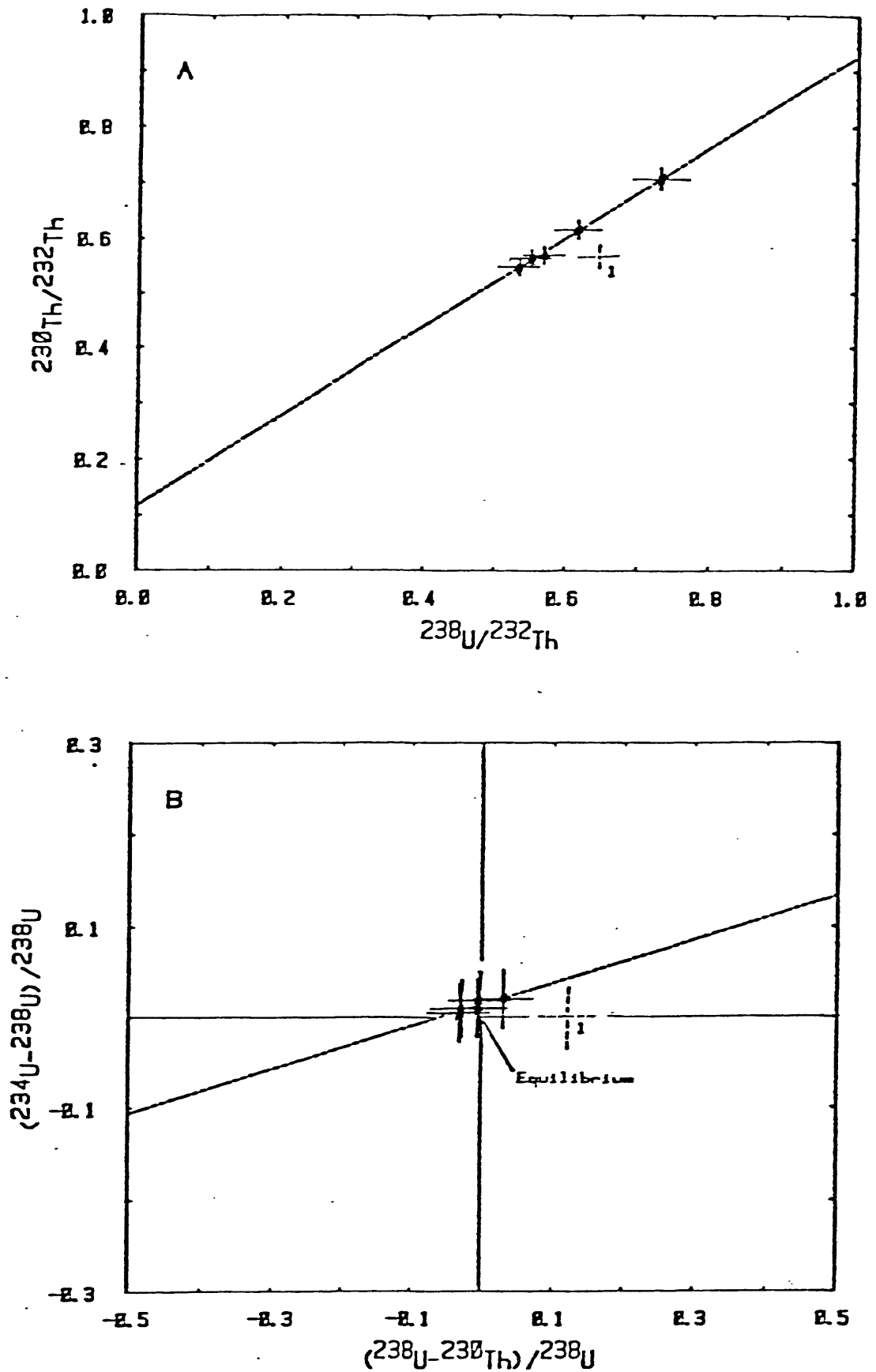


Figure 20. Plots of the upper unit of NSV3 section, loess with Pre-Bull Lake till, Boulder County, Colorado. A is Th-index, B is U-trend plot. The uppermost sample was not included in age calculation.

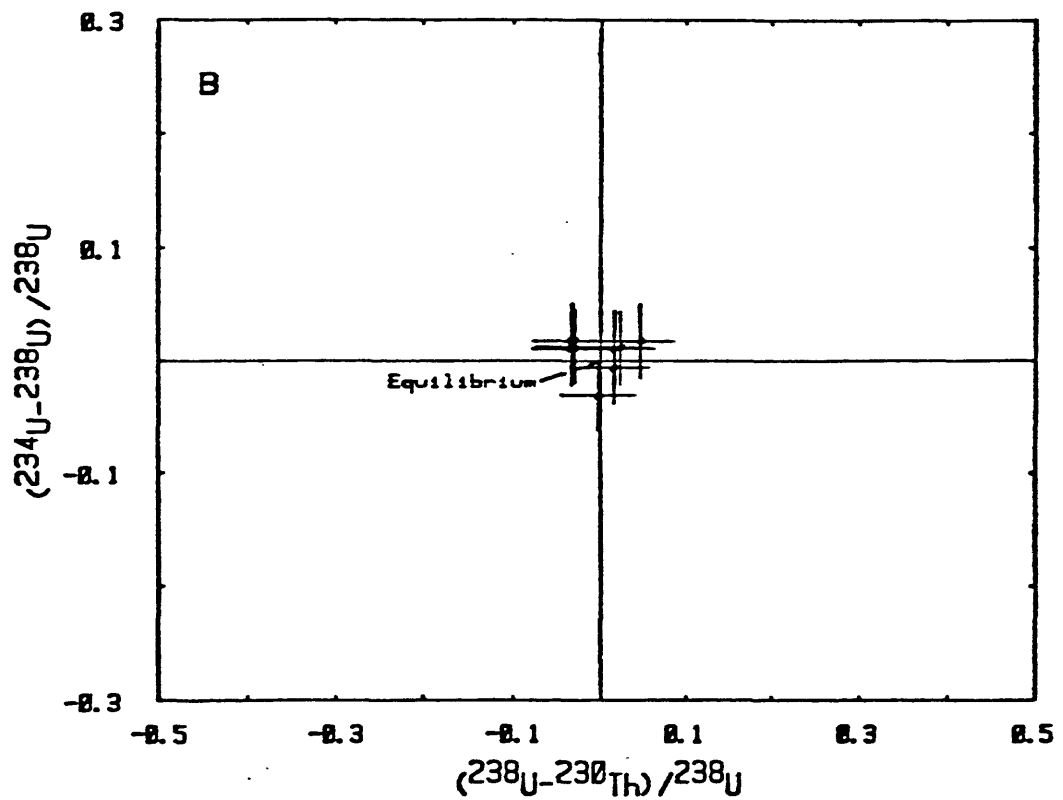
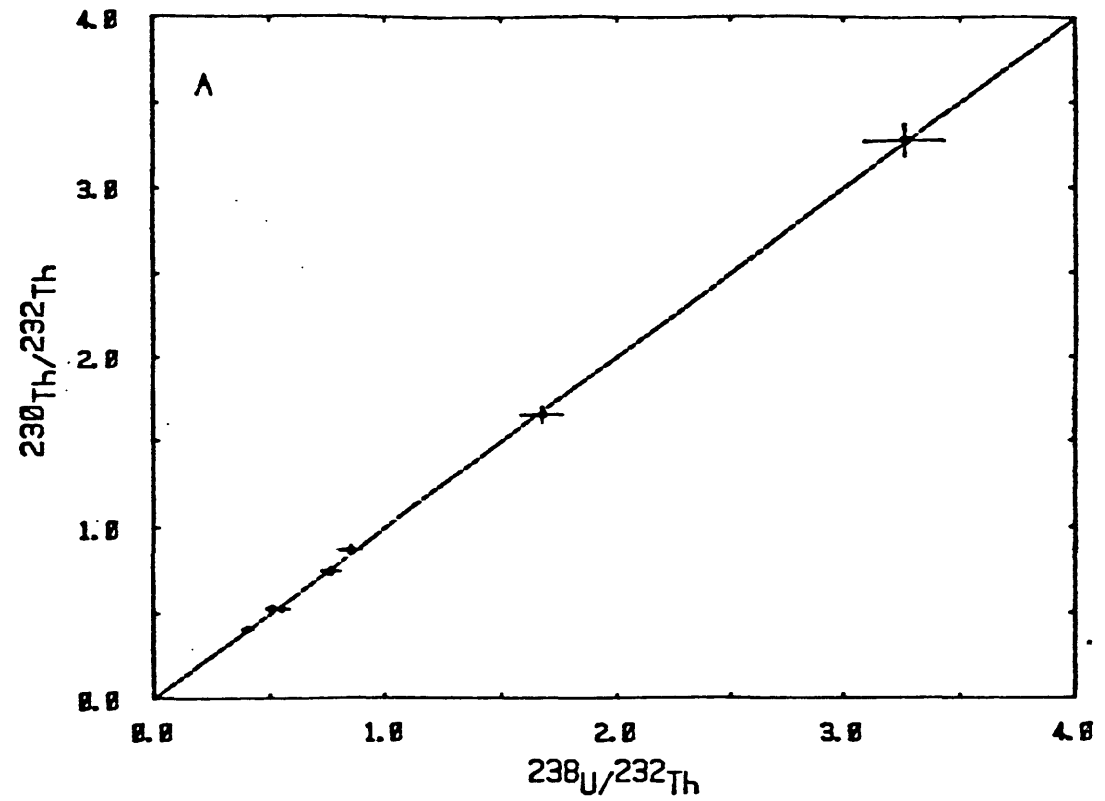


Figure 21. Plots of lower unit of NSV3 section, loess with Pre=Bull Lake till, Boulder County, Colorado. A is Th-index, B is U-trend plot. Points for U trend have insufficient spread for age calculation.

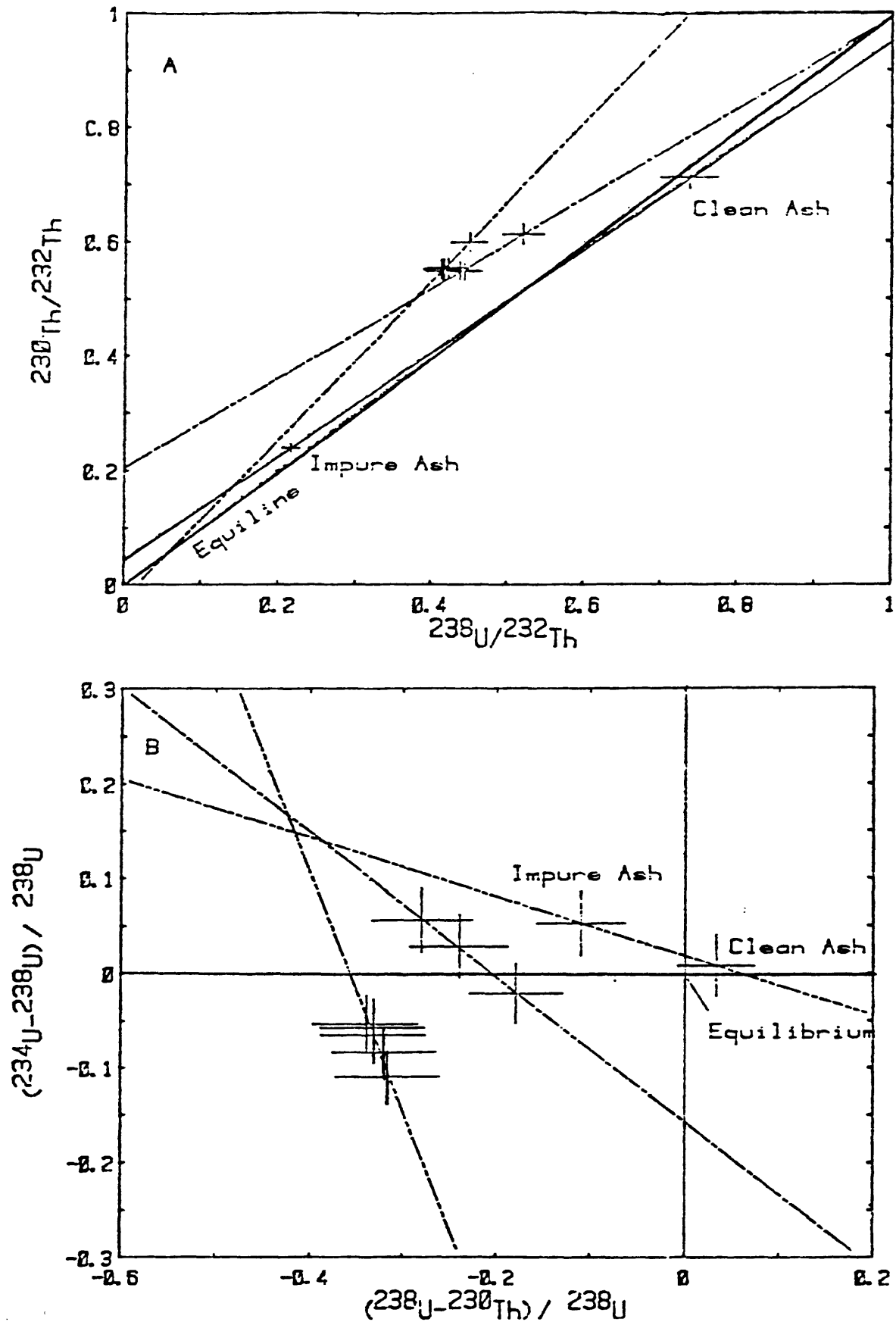


Figure 22. Plots of GF section, Golden fault zone, Colorado. Three point plots represent lower unit, five point plots represent upper unit. A is Th-indices, B is U-trend plots.